



Treball Final de Grau

Wastewater reuse using photo-Fenton process at neutral pH.

Berta Melgar Rigau

January 2024



UNIVERSITAT DE
BARCELONA

Aquesta obra està subjecta a la llicència de:
Reconeixement–NoComercial–SenseObraDerivada



<http://creativecommons.org/licenses/by-nc-nd/3.0/es/>

*El clima està canviant,
nosaltres també hauríem.*

Svante Arrhenius (1896)

Per començar, vull expressar el meu sincer agraïment a la Núria, ja que sense la seva paciència, les seves ganes d'ajudar-me i d'ensenyar-me i el seu acompanyament, avui no estaria presentant aquest treball. Vull agrair també de tot cor a totes les companyes per haver fet aquest camí juntes, especialment a les Carlotes, la Lali i la Joana, sense elles estudiar aquesta carrera no hauria estat el mateix. Per tots els plors però sobretot per tots els riures, gràcies. A les amigues, amics i companys de pis perquè sense ells haver estat lluny de casa no s'hagués sentit com estar a casa. I sobretot, moltes gràcies a la meva família, per haver confiat sempre en mi i per fer que jo també confies en mi mateixa. Per últim, però no menys important, vull agrair-me a mi mateixa per no haver-me rendit mai i per haver tirat endavant sempre, independentment de les adversitats que s'han presentat en el camí.

Moltíssimes gràcies a tots,

Berta.

CONTENTS

SUMMARY	I
RESUM	III
SUSTAINABLE DEVELOPMENT GOALS	V
1. INTRODUCTION	1
1.1. Water resources	1
1.2. Contaminants of emerging concern in water resources	2
1.3. Legislation	4
1.4. Advanced oxidation processes	6
1.4.1. History of Fenton process	8
1.4.2. Photo-Fenton process	8
1.4.3. Photo-Fenton reactions	11
2. OBJECTIVES	14
3. MATERIALS AND METHODS	15
3.1. Literature collection	15
3.2. Systematic selection of suitable articles	16
3.3. Data collection: procedures and analysis	16
3.4. Calculations	17
3.4.1. Accumulated energy	17
3.4.2. Design of the raceway pond reactor for the wastewater treatment plant at La Jonquera	18
3.4.3. Economic study for the implementation of the raceway pond reactor for the wastewater treatment plant at La Jonquera.	19
4. RESULTS	20
4.1. Artificial light	22
4.1.1. Selection of the optimal concentration of iron for the process using artificial light.	22
4.1.2. Selection of the optimal chelating agent for the process considering the water matrix and the stability of the chelating agent.	23
4.1.3. Justification of the relationship between the DOC and removal efficiencies using EDDS as chelating agent.	25
4.1.4. Comparison of the kinetics of the different micropollutants using EDTA as chelating agent.	27
4.2. Natural light	28
4.2.1. Selection of the optimal concentration of iron for the process using natural light.	30

4.2.2.	Selection of the optimal chelating agent for the process.	31
4.2.3.	Natural light using EDDS (1:1) as chelating agent, comparison of the kinetics of the different micropollutants.	33
4.3.	Design of a raceway pond reactor with the optimal parameters for the photo-Fenton process for the wastewater treatment plant in La Jonquera	34
4.4.	Feasibility study of the raceway pond reactor at the wastewater treatment plant in La Jonquera	37
5.	CONCLUSIONS	42
	REFERENCES AND NOTES	43
	ACRONYMS	47
	APPENDICES	51
	APPENDIX 1: KEYWORDS USED FOR THE RESEARCH	53
	APPENDIX 2: PRELIMINAR GRAPH OF THE INFLUENCE FT THE DOC AT THE REMOVAL USING ARTIFICIAL LIGHT	54
	APPENDIX 3: RADIATION MEASURED IN BERCELONA ON A WINTER DAY	55

SUMMARY

The photo-Fenton process is an advanced oxidation technique used to remove contaminants present in wastewater. Although the optimal pH to carry out this process is acid (approximately between 2.8 and 3), it is also studied at neutral pH. This makes the process eco-friendlier since it is not necessary to acidify and then neutralize to be able to pour the effluents into the environment. In this work of bibliographic review, the process at neutral pH has been studied with both artificial and natural light, from articles that employed chelating agents to carry it out. With artificial light has been identified what affected the process and with natural light the optimal conditions have been determined to eliminate at least 80% of the contaminants of emerging concern (CECs). The optimal conditions to eliminate the CECs, determined using natural light, since it has been considered as a more sustainable option, have been 0.1 mM of iron, 1.47 mM of peroxide and the use of EDDS as a chelating agent with a molar ratio of 1:1 with iron. Once these conditions have been identified, a raceway pond reactor (RPR) has been designed for La Jonquera Wastewater Treatment Plant (WWTP). Four different reactors have been designed, varying conditions and the criteria to choose which one has been economical. This RPR is intended to treat the water that comes out of the biological reactors, with an area of 1,169 m² and a liquid depth of 15 cm. Finally, a study has been carried out of the costs associated with the installation of this reactor in the WWTP, estimated at €218,597, considering only the installation of the reactor and the purchase of lands adjacent to the plant.

Keywords: photo-Fenton, neutral pH, wastewater treatment plant, raceway pond reactor, and contaminants of emerging concern.

RESUM

El procés foto-Fenton és una tècnica d'oxidació avançada utilitzada per eliminar contaminants presents en aigües residuals. Tot i que el pH òptim per dur a terme aquest procés és àcid (aproximadament entre 2,8 i 3), també s'estudia a pH neutre. Això, fa que el procés sigui més respectuós amb el medi ambient, ja que no és necessari acidificar i posteriorment neutralitzar per poder abocar els efluents al medi ambient. En aquest treball de revisió bibliogràfica, s'ha estudiat el procés a pH neutre amb llum artificial i llum natural, d'articles que utilitzaven agents quelants per dur-lo a terme. Amb la llum artificial s'ha identificat el que afectava el procés i amb la llum natural s'han determinat les condicions òptimes per tal d'eliminar com a mínim un 80% dels contaminants d'interès emergent (CECs). Les condicions òptimes per eliminar els CECs, determinades usant llum natural, ja que s'ha considerat com a opció més sostenible, han estat de 0,1 mM de ferro, 1,47 mM de peròxid i l'ús de l'EDDS com a agent quelant amb una relació molar d'1:1 amb el ferro. Un cop identificades aquestes condicions, s'ha procedit al disseny d'un reactor de canals obert (RPR) per a l'Estació Depuradora d'Aigües Residuals (EDAR) de La Jonquera. S'han dissenyat 4 reactors diferents variant condicions i el criteri per escollir quin es duria a terme ha sigut econòmic. Aquest RPR està destinat a tractar l'aigua que surt dels reactors biològics, amb una àrea de 1.169 m² i una profunditat líquida de 15 cm. Finalment, s'ha realitzat un estudi dels costos associats amb la instal·lació d'aquest reactor a l'EDAR, estimant-se en 218.597 €, considerant només la instal·lació del reactor i la compra de terres adjacents a la planta.

Paraules clau: foto-Fenton, pH neutre, estació depuradora d'aigües residuals, reactor de canals obert, i contaminants d'interès emergent.

SUSTAINABLE DEVELOPMENT GOALS

Els Objectius de Desenvolupament Sostenible (ODS) representen una sèrie de 17 objectius interrelacionats que van ser adoptats de manera unànime l'any 2015 per tots els estats membres de les Nacions Unides (ONU). Aquests objectius han estat concebuts amb la finalitat d'abordar els desafiaments socials, econòmics i ambientals que actualment afecten globalment la comunitat internacional, amb l'objectiu d'encaminar-se cap a un futur més sostenible.

En aquest context, la reutilització d'aigües residuals emergeix com una estratègia d'importància rellevant per aconseguir la sostenibilitat del recurs hídric. Aquesta pràctica, a més de contribuir a la reducció de la demanda d'aigua dolça, millora significativament l'eficiència en l'ús dels recursos hídrics, en conformitat amb l'ODS n° 6, referent a *aigua neta i sanejament*, mentre que alhora mitiga els impactes del canvi climàtic, tal com es contempla en l'ODS n° 13, relacionat amb *l'acció pel clima*.

La reutilització d'aigües residuals, integrada en una estratègia global de gestió de recursos i residus, contribueix de manera directa a la sostenibilitat en la producció i el consum, conforme a l'ODS n° 12, *Producció i Consum Responsables*. Aquesta pràctica, més enllà de minimitzar la contaminació, destaca per la seva capacitat per preservar la biodiversitat aquàtica i terrestre, com es contempla en els ODS n° 14 i 15, *Vida Submarina i Vida Terrestre*, respectivament. A més, emergeix com una pràctica sostenible essencial per al regadiu agrícola, contribuint a augmentar la productivitat i abordar el problema crític de la fam, segons l'ODS n° 2, *Fi de la Fam*. La gestió adequada de les aigües residuals es presenta com un element essencial per a salvaguardar la salut pública, conforme a l'ODS n° 3, *Salut i Benestar*. Així mateix, emergeix com un pilar fonamental per al desenvolupament de ciutats sostenibles i l'assegurament de l'accés universal a aigua segura, com ho estipula l'ODS n° 11, *Ciutats i Comunitats Sostenibles*.

De manera integral, aquestes interconnexions subratllen la necessitat d'abordar qüestions crucials que abracen la salut, la sostenibilitat urbana, la gestió de recursos, la conservació de la biodiversitat i la seguretat alimentària, mitjançant pràctiques sostenibles relacionades amb la gestió de l'aigua.

1. INTRODUCTION

1.1. Water resources

Water is an essential resource for life on Earth, as the survival of all living beings inhabiting it depends on it. Although water covers 70% of the planet, only 3% of the water on Earth is freshwater [1]. Over the years, the use of water has been increasing due to population growth and economic development. In consequence of the rising demand for this resource and its low availability, a concerning situation of water stress and scarcity has developed.

By the year 2050, the global population is projected to escalate from 7 billion to 9 billion individuals [2]. Consequently, in the absence of new policy implementations, the ongoing socio-economic development will precipitate the degradation and erosion of the natural environment, presenting the potential risk of irreversible changes. Because of this rise in the world population, global water demand is also expected to increase, mainly due to domestic uses, manufacturing, and electricity generation (Figure 1) [2].

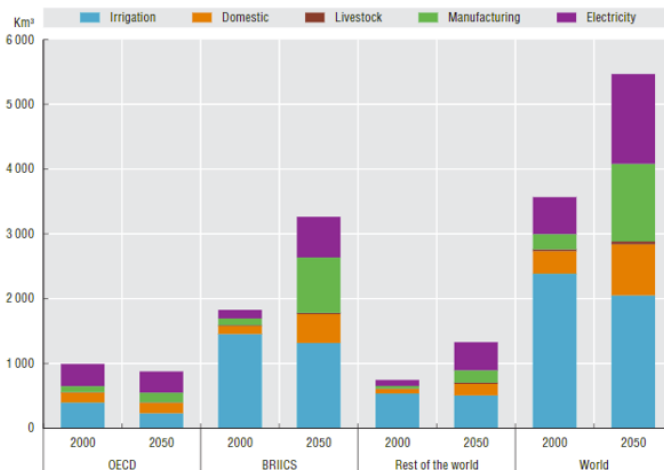


Figure 1. Predictions by 2050 of global water demands. The predictions are divided by sectors and different regions in the world, where OECD is the Organization for Economic Cooperation and Development, BRICS means Brazil, Russia, India, Indonesia, China, and South Africa [2].

The reuse of wastewater has become an important and crucial element in the sustainability of the planet. It is essential to start implementing technologies that allow the reuse of water due to the problem of the climate change, which has led to a significant drought. The scientific community has initiated an exploration for feasible technologies aimed at mitigating drought conditions, specifically targeting compounds characterized by non-biodegradable and recalcitrant properties that remain resistant to removal by conventional wastewater treatment plants (WWTPs).

1.2. Contaminants of emerging concern in water resources

In recent decades, an increase in the number of harmful pollutants has been noted, attributable to the expansion of industrial activities and population growth. The pollution of the aquatic environment is due, in part, from a diversity of contaminants of emerging concern (CECs). Although these CECs are found in very low concentrations, on the order of $\mu\text{g/L}$ to ng/L , they contribute significantly to the degradation of water quality. So, they have a negative impact, especially on human health and aqueous ecosystems [3]. CECs include several compounds such as pharmaceutical and personal care products (PPCPs), endocrine-disrupting compounds (EDCs), flame retardants (FRs), pesticides and artificial sweeteners (ASWs) [3]. These CECs can be classified by their origin, uses, potential effects to the environment or people health (Table 1).

Table 1. Classification of target CECs such as PPCPs, EDCs, FRs, pesticides, and ASWs [3].

Classes	Used	Examples
PPCPs		
Analgesics	Pain reliever	Acetaminophen and acetylsalicylic acid
Anti-epileptic drugs	Anticonvulsant	Carbamazepine and primidone
Antihyperlipidemic	Lipid regulators	Gemfibrozil, clofibrac acid, and fenofibrac acid
Non-steroidal anti-inflammatory drugs	Anti-inflammatory	Diclofenac, ibuprofen, ketoprofen, and naproxen
Synthetic hormones	Hormone	Estrone, 17 α -estradiol, 17 α -ethinylestradiol, and estriol
Antimicrobials	Antibiotic	Erythromycin, sulfamethoxazole, and tetracycline
Polycyclic musks	Antiseptic	Triclosan, biphenylol, and chlorophene
Other	Fragrances	Hexahydrohexamethyl-cyclopentabenzopyran
	Insect repellent	DEET
	Fragrances	Acetophenone
	Stimulant	Caffeine

Continuation Table 1

Classes	Used	Examples
EDCs		
Steroids	Natural human estrogen Metabolite	17 β -estradiol Estrone
Alkylphenols	Manufacture of household and industrial products	Nonylphenol and octylphenol
Polyaromatic compounds		Polychlorinated biphenyls and brominated flame retardants
Organic oxygen compounds	Plasticizers Industrial production of polycarbonates and epoxy resins	Phthalates BPA
Pesticides	Insecticides, herbicides, fungicides	Atrazine, chlordane, and trifluralin
Other	By-products of various industrial and combustion processes	Dioxins and furans
FRs		
Halogen-containing flame retardants	FRs	Brominated bisphenols and phenols
Phosphorous-based FRs	FRs	Elemental red phosphorus and inorganic phosphates
Melamine FRs	FRs	Melamine cyanurate
Inorganic hydroxides FRs	FRs	Aluminium hydroxide and magnesium hydroxide
Borate FRs	FRs	Sodium borate and boric acid
Silicone FRs	FRs	
Synergism	FRs	Halogens with antimony and phosphorus with nitrogen
Pesticides		
Carbamates	Herbicides, insecticides, and fungicide	Carbendazim, benomyl, and carbaryl
Chloroacetanilides	Preemergent herbicides	Metolachlor and alachlor
Chlorophenoxy acids	Herbicides	Bentazone and triclopyr
Organochlorines	Insecticides	DDT, dieldrin, endrin, and endosulfan
Organophosphates	Insecticides	Diazinon, malathion, and chlorpyrifos
Pyrethroids	Insecticides	Biphenthrin, cypermethrin, and esfenvalerate
Triazines	Herbicides	Atrazine, cyanazine, and simazine
Other pesticides		Phenylurea herbicide isoproturon and mecoprop
ASWs		
Artificial sweeteners	Sugar substitutes	Acesulfame Sucralose Saccharin Cyclama Aspartame Neotame Neohesperidine dihydrochalcone

As mentioned earlier, the presence of compounds in water endangers human health and the environment. Fortunately, these contaminants can be removed through advanced oxidation processes (AOPs). However, before that, legal regulation of these CECs must be developed to establish limits for water quality. Unfortunately, as of today, this is still a developing issue, as existing legislation is insufficient given the current challenges. Only a negligible number of CECs are regulated, delaying the development and implementation of new technologies to enhance water quality and facilitate its reuse [4].

1.3. Legislation

In recent times, with globalization and socioeconomic growth, new microcontaminants have been discovered. For this reason, new technologies are being developed to address their removal. Only a small fraction of these contaminants is currently covered by the actual legislation (Figure 2); there is, therefore, an urgent need for genuine regulation, as many of these compounds are being released into aquatic environments and are harmful [4].

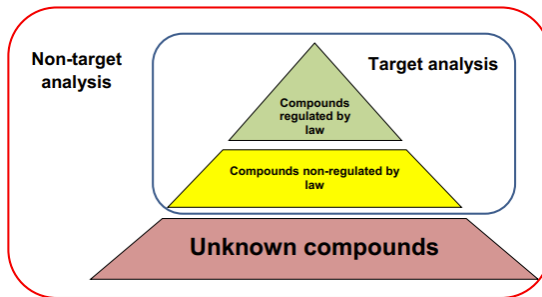


Figure 2. Type of compounds found in the aquatic environment [4].

In accordance with the various purposes assigned to treated water in WWTPs, the relevant legislation must be specific, considering the potential variations in its utilization. Given the current situation of significant drought, an alternative of notable interest for treated water lies in its capacity for reuse. The current regulations are restrictive depending on the intended use of the reused water. Although there are numerous possibilities for the reuse of treated wastewater, agricultural reuse is the most widespread practice.

The regulatory frameworks overseeing water treatment typically prioritize the elimination of organic matter, suspended solids, and pathogenic microorganisms. Notably, there has been a

recent escalation in the prevalence of persistent organic compounds within secondary effluents, recognized as CECs. Despite their presence in the environment at exceedingly low concentrations, these compounds pose a threat to both human health and the environment due to their bioaccumulative nature. Furthermore, conventional treatments administered in standard WWTPs prove inadequate for their complete removal [3, 5].

In the European Union (EU) the concern for water quality have increased in recent years. Since the ability to respond to the increasingly growing water pressure could be enhanced through greater reuse of treated water, legislation for that has been reviewed. Legal regulations currently only include substances found in the environment in more common and significant concentrations, so it is important to start regulating since all these compounds end up in aquatic environments [4].

The European Parliament took measures to combat water pollution through Directive 2000/60/EU. The Commission presented a list of priority substances posing a significant risk to aquatic environments, establishing a priority order for measures to be taken with these microcontaminants [6].

In May 2020, the European Commission approved a new regulation (EU 2020/74) to address water scarcity and the consequent pressure on water resources in a coordinated manner throughout the Union [6, 7]. This regulation establishes minimum quality and control requirements for water to ensure that regenerated waters are safe for agricultural irrigation, thereby promoting circular economy practices and adaptation to climate change. It also contributes to the objectives of the before mentioned Directive 2000/60/EU [7]. In this new regulation, different quality classes (class A, B, C, and D) are defined depending on the intended reuse of the water.

On May 11, the EU published Royal Decree-Law 4/2023, which, among other matters, adopts urgent measures related to water in response to the current drought. This regulation promotes the use of reclaimed water in agriculture by establishing certain parameters to ensure the safety of water reuse in agricultural irrigation [8, 9]. While it is true that the reuse of treated water is implemented in some member states, in the EU, only 2.4% of the total treated urban wastewater is recovered and reused. This data highlights the considerable potential for a more efficient utilization of water [8].

1.4. Advanced oxidation processes

As a consequence of the recalcitrant nature of the CECs and their low concentrations, they cannot be completely eliminated by conventional treatments applied in conventional WWTPs. Among the new technologies available for wastewater regeneration, AOPs deserve special mention for their high efficiency. These offer an effective means of addressing recalcitrant contaminants, which are substances resistant to elimination through conventional treatment methods. While AOPs demonstrate the capacity to convert contaminants into biodegradable intermediates or achieve complete mineralization (conversion to CO₂) [11], it is imperative to acknowledge certain limitations associated with their application, including the consumption of energy and chemicals, as well as potential increases in treatment time and cost [12].

AOPs are methods based on the generation of hydroxyl radicals, which subsequently react to achieve the effective removal of microcontaminants [1]. The selection of the appropriate AOP depends on the specific treatment needs of wastewater and the contaminant intended for removal.

In Catalonia, water sanitation systems in operation allow for the treatment of wastewater from 97% of the population [53], and various tertiary treatments are implemented to regenerate water. The treatments implemented in water regeneration stations in Catalonia include chlorination, ultrafiltration, reverse osmosis, coagulation, among others (Figure 3).

However, none of these plants utilizes the photo-Fenton process for water regeneration and subsequent reuse. Since this process is not implemented and is notably effective, particularly due to the generation of hydroxyl radicals and use of UV light, which is economic and ecofriendly, it is proposed as a subject of study for implementation in a WWTP in Catalonia. The purpose of this research is to assess the viability and effectiveness of the photo-Fenton process as an option to improve water resource management in the region, with the aim of promoting sustainability and water reuse. Therefore, it serves as an alternative to conventional treatments [5]. The solar photo-Fenton process has stood out because of its high efficiency in terms of decontamination and disinfection, and for that reason is one of the most studied AOPs now [11].

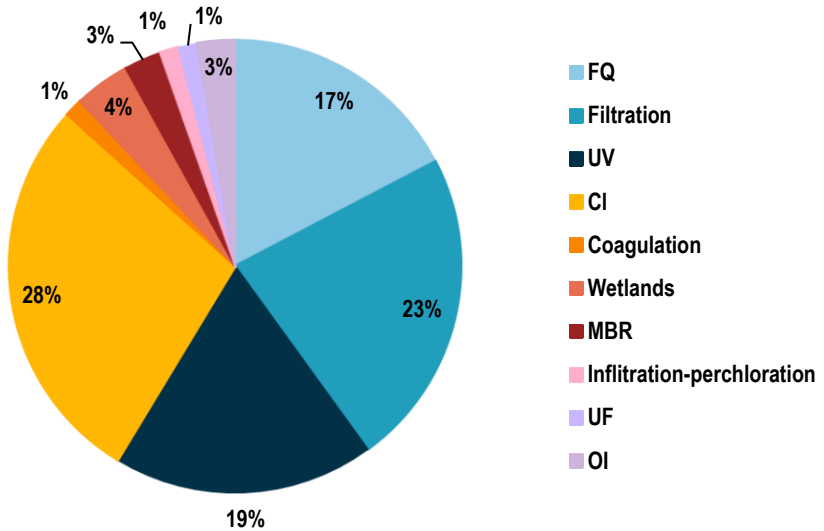


Figure 3. Treatments used at public water regeneration stations in Catalonia.

FQ: physico-chemical treatment, CI: chlorination, UV: ultraviolet disinfection, MBR: membrane bioreactor, UF: ultrafiltration, OI: reverse osmosis [53].

The Fenton process and the photo-Fenton process are two variants of wastewater treatment that involve the degradation of organic contaminants using advanced chemical reactions, but they differ in how the oxidation reaction is activated. In the conventional Fenton process, the activation of the reaction is achieved by adding a specific amount of iron ions and hydrogen peroxide to an aqueous solution. It is not necessary to use UV radiation or another external energy source to activate the reaction. In contrast, the photo-Fenton process is a variation of the Fenton process that incorporates UV as an external energy source. By exposing the Fenton solution to UV radiation, more hydroxyl radicals are generated, which increases the speed and efficiency of organic contaminant oxidation [1]. Both processes are used to treat contaminated wastewater, but the photo-Fenton process is considered a more advanced and efficient option in terms of decontamination and disinfection [23].

The photo-Fenton process is a homogeneous photocatalytic process (the catalyst and the reactants are in the same phase) used for wastewater treatment, that uses UV light and hydrogen peroxide in the presence of iron to break down organic contaminants. The

combination of these reagents generates highly reactive free radicals that oxidize and degrade compounds and, consequently the water is purified [22].

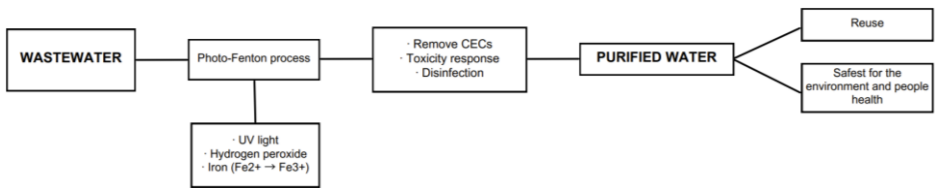


Figure 4. Schematic representation of wastewater reuse using photo-Fenton process [own elaboration].

1.4.1. History of Fenton process

The photo-Fenton process is based on the Fenton reaction which was discovered by Henry John Horstman Fenton in 1894. Fenton noticed that the combination of hydroxide peroxide (H_2O_2) and iron ions (Fe^{2+} or Fe^{3+}) generated hydroxyl free radicals (OH^\bullet) known for being highly reactive and capable of oxidizing a wide range of organic compounds [1].

Over time, efforts were made to explore ways to improve the efficiency of the Fenton reaction. Between the 1990s and 2000s, the idea of using UV light came up. The UV activates H_2O_2 and accelerates the formation of OH^\bullet , thereby increasing the degradation of contaminants [1, 10].

As the benefits of the photo-Fenton process became better understood, it began to be employed for environmental purposes, becoming a tool in the fight against water pollution and the treatment of contaminated wastewater. Currently, research is ongoing to improve the efficiency of the process, reduce its costs, and adapt it to a variety of conditions and types of contaminants.

1.4.2. Photo-Fenton process

As mentioned earlier, the photo-Fenton process involves the variation of the Fenton process by adding UV light, which increases the production of OH^\bullet , thereby enhancing the efficiency of microcontaminant removal. This increase in process efficiency is achieved through the

photoreduction of Fe^{3+} to Fe^{2+} , leading to a redox cycle that results in the continuous generation of OH^\bullet radicals (Figure 5).

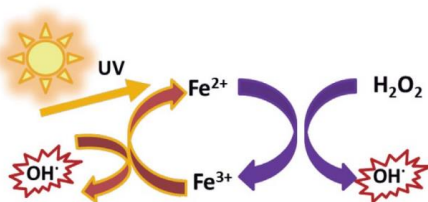


Figure 5. Cycle redox scheme in the photo-Fenton process [5].

There are several parameters that influence the effectiveness of the photo-Fenton process, pH and temperature, concentration of Fenton reagents and of the pollutants (water matrices).

➤ pH

This is a key factor for the process, as depending on the pH at which it is working, iron will be found in solution in one way, or another as can be seen in Table 2.

Table 2. Forms of iron depending on the pH [1].

pH	< 2.3	2.3 – 3.5	> 3.5
Ferric ion	$[\text{Fe}(\text{H}_2\text{O})_6]^{3+}$	FeOH^{2+}	$[\text{Fe}(\text{H}_2\text{O})_4(\text{OH})_2]^+$ and $[\text{Fe}(\text{H}_2\text{O})_3(\text{OH})_3]$
Characteristics	Low reactivity with H_2O_2	Higher absorption of UV and is soluble	Low solubility, they precipitate

The optimal pH for carrying out the process is 2.8; however, this poses certain inconveniences, as the water needs to be acidified before and neutralized afterward to be discharged into the environment [28]. For this reason, there is an interest in researching the development of the process at neutral pH, thus avoiding the need to adjust the pH before and after the process. As observed in Table 2, at neutral pH, iron precipitates, significantly reducing the efficiency of the process. However, there is a solution to this issue, which involves adding compounds capable of forming stable complexes with iron ions [27]. These compounds are called chelating agents and are what allow us to develop the photo-Fenton process at neutral pH. These agents function to prevent the precipitation of iron at neutral pH by forming stable complexes with it. In this manner, iron remains in solution and is available to undergo the necessary chemical reactions for the removal of microcontaminants. Consequently, they contribute to enhancing the efficiency of the process under conditions approaching neutrality.

Fe^{3+} forms very stable complexes with aminopolycarboxylic acids (APCAs) in a large pH range, these APCAs are ligands that can form stable water-soluble complexes with metal ions [32, 34]. Some of the most APCAs used are ethylenediaminetetraacetic acid (EDTA), ethylenediamine-N,N'-disuccinic acid (EDDS), nitrilotriacetic acid (NTA) and, diethylene triamine pentaacetic acid (DTPA).

➤ Temperature

Temperature contributes in two ways to the process. An increase in temperature accelerates the decomposition Iron-chelate complex due to its instability at neutral pH, but simultaneously enhances the Fenton reaction [26]. This occurs because, following Arrhenius principle, a rise in temperature is anticipated to lead to an augmentation of the reaction rate constant and consequently in a higher generation of hydroxyl radicals [13]. Considering this, it is imperative to maintain the temperature below 50°C , as exceeding this threshold leads to the thermal decomposition of H_2O_2 . This decomposition diminishes the production of hydroxyl radicals and, consequently, reduces the oxidative capacity in solution [1, 13]. Therefore, the process is conventionally conducted within the temperature range of approximately 20 to 40°C [1, 13, 26].

➤ Reagents concentration

Increasing the concentrations of iron and hydrogen peroxide has a positive impact on the efficiency of the process. However, this effectiveness is subject to the specific ratio maintained between the reagents. The optimal ratio is contingent upon factors such as water quality and the intended purpose of water reuse [1]. It is imperative to carefully consider and adjust this ratio to achieve the desired treatment outcomes, ensuring both efficiency and effectiveness in the context of the water treatment process.

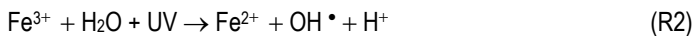
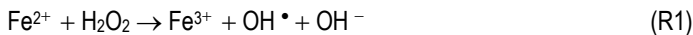
➤ Water matrix

The composition and characteristics of organic matter play a pivotal role in the degradation of CECs within WWTPs. The inherent properties of this organic matter within WWTP effluents significantly influence the kinetics of degradation under specified treatment conditions [25]. Various water matrices, such as Integrated Fixed-Film Activated Sludge (IFAS), Conventional Activated Sludge (CAS), Membrane Bioreactor (MBR), and Conventional Activated Sludge with nutrient elimination (CAS-NE), present diverse physicochemical attributes, particularly in terms of organic matter content, turbidity, and alkalinity [33].

IFAS and CAS matrices exhibit elevated levels of organic matter and turbidity, while MBR and CAS-NE matrices demonstrate comparatively lower values for these parameters [29]. Importantly, it has been established that matrix with heightened organic load and turbidity experience diminished removal efficiencies. This reduction can be attributed to the inherent complexity of the matrix, wherein organic matter absorbs a portion of the radiation reaching the reactor [29, 33]. Therefore, understanding the nature of organic matter in different water matrices is crucial for predicting and optimizing the degradation kinetics of CEC within wastewater treatment processes.

1.4.3. Photo-Fenton reactions

As previously mentioned, the neutral pH photo-Fenton process represents an intriguing alternative to address a significant drawback of the acidic pH-dependent Fenton process. The conventional approach requires prior acidification and subsequent neutralization, adding complexity to the treatment [35]. At acidic pH, the mechanism primarily involves the Fenton reaction (R1), characterized by the oxidation of Fe^{2+} to Fe^{3+} in the presence of H_2O_2 . Additionally, the photoreduction of Fe^{3+} to Fe^{2+} , accelerated by UV radiation (R2), closing the redox cycle [23].



At neutral pH, this treatment can be implemented either homogeneously or heterogeneously, depending on the nature of the catalyst. In the homogeneous approach at neutral pH, the process employs chelating agents. The reactions involved remain analogous to those in the conventional Fenton process, with the notable inclusion of chelating agents. These reactions are as follows [23, 24].



Maintaining an appropriate molar ratio between iron and the ligand is a crucial parameter in the process. This ratio is imperative for achieving optimal performance and ensuring the

successful chelation of iron, which is pivotal for the effective degradation of targeted pollutants [22].

The reactions of the photo-Fenton process are carried out at photoreactors. The photoreactors commonly used in solar applications come in the form of tubular reactors with compound parabolic collectors (CPC) [22, 15]. These collectors efficiently accumulate direct and diffuse solar radiation, focusing it onto the tubes. The suitability of CPC reactors lies in their ability to operate at high iron concentrations (on the order of tens of mg/L), attributed to the high demand for photons required for the photo-reduction of ferric iron, the absorbing species, transforming it into ferrous iron. This process effectively closes the photo-Fenton redox cycle, especially in the treatment of wastewater containing contaminants in the range of hundreds of mg/L [15].

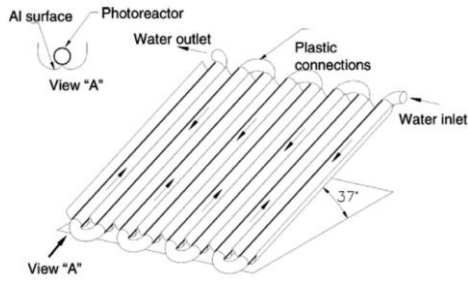


Figure 6. Schematic diagram of CPC [17]

Several years ago, the proposal was put forth to use low iron concentrations (≤ 5 mg/L) for the removal of micropollutants through the photo-Fenton process. This approach, characterized by a lower requirement for OH^\bullet and the avoidance of iron removal in subsequent treatment, allows for the direct reuse of water for irrigation. A notable result of this strategy is the feasibility of using reactors that, while capturing light less efficiently than CPCs, are more cost-effective. Among them, the raceway pond reactor (RPR) stands out, consisting of open channels through which water is moved by a paddle wheel [15].

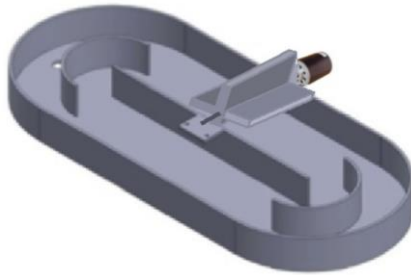


Figure 7. Schematic diagram of RPR [18].

It is estimated that the cost of installing a large-scale CPC for solar photo-Fenton is €400/m². Therefore, to bring the application of this solar treatment closer to an industrial scale, the adoption of low-cost reactors such as RPRs, with significantly lower construction costs (approximately €10/m²), could be a more viable option [16].

RPRs, in addition to having a lower cost than CPCs, are also characterized by their high treatment capacity and their ability to vary the liquid depth depending on the available UV radiation [14]. However, there is a gap in the implementation of this type of reactor at a large scale, emphasizing the importance of continuing to explore and optimize the operation of RPRs in continuous mode at the pilot scale, paving the way for a successful commercial implementation of the photo-Fenton process for wastewater reuse [23].

2. OBJECTIVES

The main objective of this work is to carry out a literature review of the photo-Fenton process at neutral pH to remove contaminants of emerging concern contained in urban wastewater.

Based on this review, sub-objectives are established, which are:

1. Study how different parameters affect the efficiency of the process, and determine the optimal conditions in terms of oxidant, catalyst, and radiation.
2. Realize a study for the implementation of this technology at the wastewater treatment plant in La Jonquera.
3. Conduct an economic study for the implementation of this technology at the wastewater treatment plant in La Jonquera.

The three sub-objectives are closely interconnected because, starting with the first one, by optimizing the different variables, we can design the photo-Fenton process plant, depending on the design of that plant, we can then assess its economic feasibility.

3. MATERIALS AND METHODS

In this section, it is detailed the systematic protocol followed to carry out this research work. It includes four main stages: literature collection (Section 3.1), systematic selection of suitable articles (Section 3.2), data collection (Section 3.3), and calculations (Section 3.4).

3.1. Literature collection

An exhaustive search was conducted using the Web of Science and Scopus databases during September and October of 2023. The search procedure involved the utilization of advanced search techniques employing keywords (Appendix 1) relevant to the objectives of this research. The keywords used for the search and the number of articles related to them are presented in Figure 8. The search began with a specific inquiry and subsequently expanded to a more expanded investigation.

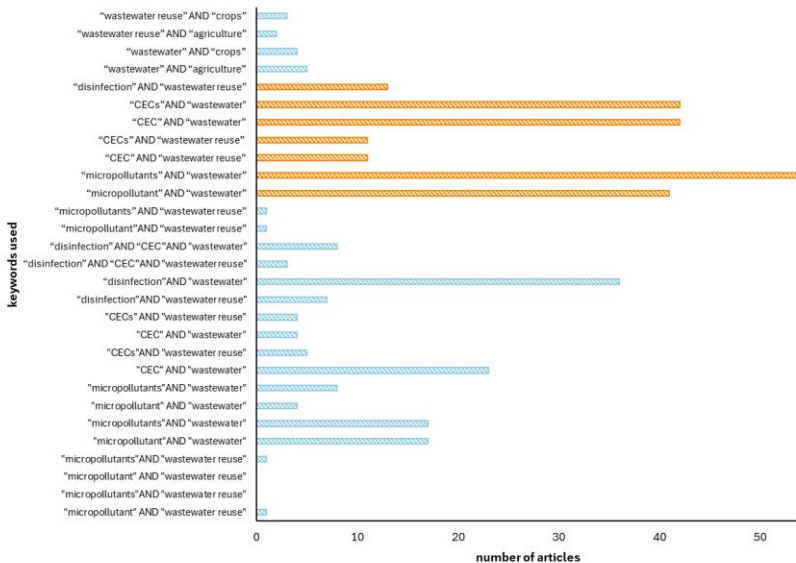


Figure 8. Number of manuscripts found in the initial search. All the searches have the keyword photo-Fenton, the blue ones take into account the pH, whereas the orange ones do not [own elaboration].

The initial phase of the search supplied a total of 140 articles, which were subsequently subjected to rigorous filtration and selection processes. The specific criteria applied during this selection process are detailed in Section 3.2 of this work. Following the systematic selection procedure, 31 articles were identified as suitable for the completion of this study. These selected articles served as the source of data for the development of this research work. Additionally, elaboration on the criteria employed for data extraction from these articles can be found in Section 3.3. And finally, in Section 3.4 can be found all the calculations used for the realization of the work.

3.2. Systematic selection of suitable articles

For the selection of articles of interest for the development of the work, the abstracts and conclusions of each article were read, and if necessary, the entire article was read. Various aspects were considered to decide if an article was to be selected or not. Some of these aspects included the pH used, if data on accumulated energies and efficiencies could be extracted for shorter time intervals than the total treatment time, also if chelating agents were used or not... For instance, all articles had to carry out the process at neutral pH and use chelating agents. In other words, if an article conducted the process without a chelating agent, it was discarded. If it did use one, it was noted on the list, and all the data of interest for the subsequent development of results were extracted.

3.3. Data collection: procedures and analysis

The data related to the objective of this work were collected from the selected articles (section 3.2) and organized in a Microsoft® Excel database. The articles were reviewed and the necessary information of each one was noted in the Excel datasheet.

The data extracted from the articles consisted of information relevant to the fulfilment of the objectives of this study. To achieve this, it was imperative to identify the nature of the effluent under investigation and its specific characteristics. Additionally, details about the concentrations of iron and hydrogen peroxide employed in the treatment were also extracted, as well as the type of chelating agent used and its molar ratio with iron. It was also important to identify the contaminant or contaminants targeted for removal. Furthermore, the type and quantity of

radiation were also noted whether it was natural or artificial, along with specifics related to the type of reactor and its characteristics, and the duration of the treatment process.

3.4. Calculations

To achieve the objectives of this work, various calculations were carried out. Firstly, the calculation of the accumulated energy for each article was performed (Section 3.4.1). Subsequently, once the process parameters were optimized, the design of a raceway pond reactor was undertaken (Section 3.4.2). Finally, after the design of this reactor, an economic feasibility study was conducted (Section 3.4.3).

3.4.1. Accumulated energy

To achieve the first objective of finding the optimal conditions for carrying out the process, it was necessary to standardize the elimination efficiency results of different articles [1]. The parameter used to standardize the results was the accumulated energy (Q_{uv}), which includes the treatment time, the radiation reaching the reactor, and its dimensions. Using the data extracted from each article, which included radiation reaching the reactor surface (I), reactor area (A), treatment time (t), and treated volume (V), and applying conversion factors considering the corresponding units, the Q_{uv} energy was calculated using equation 1.

$$Q_{uv} \left[\frac{\text{kJ}}{\text{L}} \right] = \frac{I \left[\frac{\text{J}}{\text{m}^2} \right] \cdot A \left[\text{m}^2 \right] \cdot t \left[\text{s} \right]}{V \left[\text{L} \right]} \cdot \frac{1 \text{ kJ}}{10^3 \text{ J}} \quad (\text{Eq. 1})$$

Once the results of the articles were standardized, the limiting Q_{uv} was identified and used to extract all elimination efficiencies of contaminants, allowing for coherent comparisons.

3.4.2. Design of the raceway pond reactor for the wastewater treatment plant at La Jonquera

For the development of the reactor design, the first step involves calculating its design area. This will be determined by the design flow rate, the selected Q_{uv} for the process, and the radiation reaching the surface (Equation 2).

$$A_{RPR} = \frac{Q_{uv} \cdot V}{I \cdot t} = \frac{Q_{uv} \cdot Q_{design}}{I} \quad (\text{Eq. 2})$$

Through bibliographic research, relationships between the dimensions of the RPR were identified, allowing for the dimensioning of the reactor based on the known area (Equations 3, and 4) [14, 19]. Where L_T is the total length of the reactor, L is the length of the wall within the channels and W is the width of the channel.

$$L_T = L + 2 \cdot W \quad (\text{Eq. 3})$$

$$\frac{L_T}{W} = 10 \quad (\text{Eq. 4})$$

To solve these equations and find the dimensions, it was proposed that the previously determined area with Equation 2 could be expressed as in Equation 5.

$$A_{RPR} = A_{rectangle} + A_{circle} = (L \cdot W) + (\pi \cdot R^2) \quad (\text{Eq. 5})$$

Since the radius is equal to the channel width, and the ARPR is already calculated with Equation 2. Using equations 3, 4, and 5 we can find the radius (R), and consequently the channel width (W). Once these are found, the lengths can also be calculated.

Once the reactor has been dimensioned, through the application of equation 6 [19], we can determine the width (t) of its walls. The height of the walls is the H , and the liquid depth is the LD .

$$t = H - \frac{V}{A} = H - \frac{A \cdot LD}{A} = H - LD \quad (\text{Eq. 6})$$

Subsequently, with the knowledge of the width obtained through equations 7, 8, 9, and 10, we can derive the various sections [19], which, in turn, will enable us to determine the total reaction area (Equation 11). An scheme of the different sections is showed in Figure 9.

$$S_1 = \frac{\pi \cdot R^2}{2} \quad (\text{Eq. 7}); S_2 = L \cdot W \quad (\text{Eq. 8}); S_3 = L \cdot t \quad (\text{Eq. 9}); S_4 = \frac{\pi \cdot (\frac{R}{2} + \frac{t}{2})^2}{2} \quad (\text{Eq. 10})$$

$$S_{\text{reaction}} = 2 \cdot S_1 + S_2 - S_3 - 2 \cdot S_4 \quad (\text{Eq. 11})$$

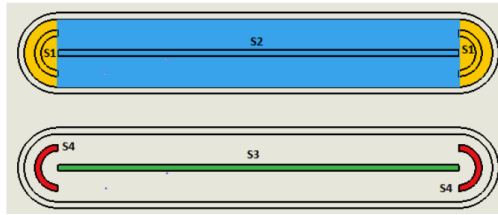


Figure 9. Scheme of the different sections of the RPR [19].

With these equations, various reactors are dimensioned since their design will depend on the radiation they receive and the liquid depth, among other variables. Subsequently, after the economic study conducted, a decision will be made regarding which one to opt for construction at the WWTP in La Jonquera.

3.4.3. Economic study for the implementation of the raceway pond reactor for the wastewater treatment plant at La Jonquera.

For the realization of the economic feasibility study calculations, two factors have been taken into consideration. Firstly, the quantity of material required for the construction of the reactor was considered, and secondly, the additional amount of land necessary for its construction was considered.

Regarding the cost of construction material, which is expressed in relation to cubic meters of material, the volume of walls and ground has been calculated (Equations 12 and 13) to subsequently convert it into the corresponding price.

$$V_{\text{RPR,walls}} = (2 \cdot t \cdot L \cdot H) + (\pi \cdot R \cdot t \cdot H) + (t \cdot L \cdot H) + \left(\pi \cdot \left(\frac{R}{2} + \frac{t}{2} \right)^2 \cdot H \right) \quad (\text{Eq. 12})$$

$$V_{\text{RPR,floor}} = (t \cdot L \cdot 2 \cdot W) - (L \cdot t^2) + (\pi \cdot R^2 \cdot t) - \left(2 \cdot R \cdot \pi \cdot \left(\frac{R}{2} + \frac{t}{2} \right)^2 \right) \quad (\text{Eq. 13})$$

In contrast, the cost of the additional land required for construction has been determined based on square meters of land. Therefore, the additional land area required has been calculated to perform the conversion to price.

$$A_{\text{ampliation}} = L_{\text{ampliation}} \cdot W_{\text{ampliation}} \quad (\text{Eq. 14})$$

The total cost of the reactor construction is defined as the sum of the construction costs and the additional land required.

4. RESULTS

With the bibliographic research carried out, it has been possible to observe that there are different factors that influence the elimination of microcontaminants, and all of them must be considered when choosing the optimal conditions for treatment. In the case of the studied process, it is necessary to consider the pH, which is related to chelating agents. Also, the concentrations of the reagents, both iron and peroxide are important, and it is crucial to consider the ratio between these two compounds. Finally, the type of water matrix to be treated also has an impact.

The photo-Fenton process is significantly pH-dependent, as the initial pH has a substantial influence on the production of hydroxyl radicals. As previously highlighted, the optimal pH for the process is acidic. However, when implemented at an industrial level, it is preferable to conduct the process at a neutral pH using chelating agents. This avoids the need to acidify the initial solution and subsequently neutralize it before releasing it into the environment [41]. Additionally, it is crucial to consider the concentrations of the reagents, both iron and peroxide, and the ratio between these two compounds. More relevant than the individual concentration of each reagent is, in fact, the ratio between them. If the ratio between iron and hydrogen peroxide is balanced and there is no excess reactant, it can be ensured that both reactants actively participate in the process. If one of the reactants is in excess, it may remain unused, thereby reducing the effectiveness of the process and increasing the production of undesired byproducts. For this reason, the ratio between iron and hydrogen peroxide is crucial, and the higher this ratio, the greater the efficiency of the process [43].

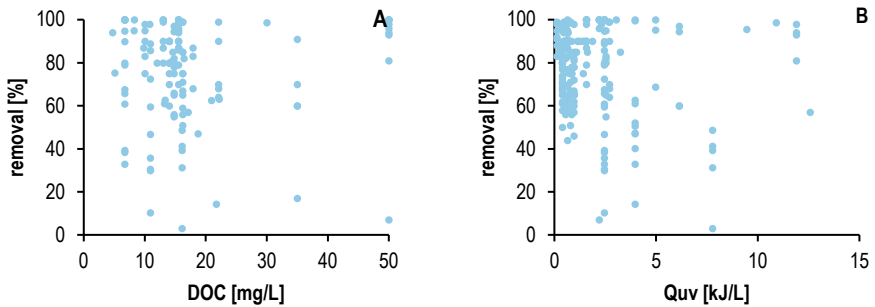


Figure 10. How DOC (A) and how Q_{UV} (B) affects the removal of CECs without considering any variable.

Moreover, the characteristics of the water matrix to be treated also play a significant role in the process. The specifics of each type of water matrix are diverse, and these discrepancies directly influence the micropollutants removal process. One of the most used parameters to characterize water is the Dissolved Organic Carbon (DOC). As water contains less organic matter, it will be less competence for the hydroxyl radical within DOC and CECs, so more CECs will be eliminated [20].

Figure 10-A represents the influence of DOC at the final efficiency of the treatment performed, without considering any variables. In other words, they compare the results of all the articles, even if they do not use the same operation conditions. The figure 10-B represents the influence of the Q_{UV} in the removal efficiency, also without considering any variables. Given that it does not make sense to compare disparate results without considering the variables employed, as illustrated in Figure 10, a decision has been made to select specific variables to facilitate a coherent comparison of the results obtained. This approach enables the development of conclusions regarding the optimal parameters for executing the process.

The impossibility of directly comparing the articles is acknowledged, leading to their grouping based on established ranges of various variables. A primary criterion for differentiation was the type of lighting used, distinguishing between those employing artificial light and those utilizing natural light. This distinction is justified by the differing characteristics of both types of light, making it inappropriate to compare elements that are unrelated. Additionally, ranges of iron concentrations were established, and articles were classified within each range based on the chelating agent used. Articles were separated in ranges with the aim of optimizing the

search for the optimal conditions to the process, enabling a more coherent comparison of the obtained results.

One of the critical variables influencing the process is the Q_{UV} , which has been standardized to allow for the comparison of elimination efficiency values, considering other influential parameters such as DOC, concentrations of iron and hydrogen peroxide, or chelating agent, that also exert significant influence on the development of the process. This normalization of Q_{UV} facilitates the understanding and evaluation of the overall system effectiveness, as it enables a relative analysis of elimination efficiency concerning multiple critical variables affecting the treatment process.

4.1. Artificial light

Articles 20, 21, 28, 29, 31, and 33 are the ones using artificial light, in Table 3, it can be observed, for each article, the CECs removed, the chelating agents employed for removal, and the concentrations of both iron and peroxide.

Table 3. Main conditions of each article using artificial light

n° article	CECs	chelating agent	iron [mM]	peroxide [mM]
20	Propranolol	EDDS and EDTA	0.18	4.41
21	Propranolol, sulfamethoxazole, acetamiprid	EDDS and EDTA	0.089	1.47
28	Acetamiprid	EDDS	0.1	0.88
29	Propranolol	EDDS and EDTA	0.18	4.41
31	Amoxicilin and acetaminophen	EDDS	0.098	0.147
33	Propranolol, sulfamethoxazole, acetamiprid	EDDS and EDTA	0.089	1.47

4.1.1. Selection of the optimal concentration of iron for the process using artificial light.

For the corresponding analysis, it was decided to define two ranges of iron concentrations, as the articles using artificial light employed iron concentrations ranging from 0.089 to 0.18 mM. The first range comprises articles working with concentrations from 0 to 0.1 mM, and the second

includes those working with concentrations from 0.1 to 0.18 mM. Since one of the criteria used to compare results is the ratio between iron and hydrogen peroxide, concentration ranges for hydrogen peroxide are not established, as it is already included in this ratio. Between these two concentration ranges, the decision is made to stick with the first one (0-0.1 mM). This choice is based on the observation of elimination efficiencies between waters with similar DOC and the removal of the same microcontaminant (propranolol), where there is not much difference as can be seen in Table 4. Therefore, for purely economic reasons, it is decided that with artificial light, it is preferable to use an iron concentration of 0.1 mM. This way, less reagent will be expended.

Table 4. Comparative of the elimination efficiencies to choose the optimal range using artificial light. Range 1 [Fe] = 0 - 0.1 mM and range 2 [Fe] = 0.1 - 0.18 mM

Range 1			Range 2		
Article	DOC	Removal [%]	Article	DOC [mg/L]	Removal [%]
21	6.7	82	20	4.7	87
33	10.9	30	29	13.2	20

Once the choice of concentration range is justified, the next step is to analyse and justify the results obtained for this range.

4.1.2. Selection of the optimal chelating agent for the process considering the water matrix and the stability of the chelating agent.

The selection between the two chelating agents has been carried out in the context of the process, and this decision is grounded in the data obtained from Article 33, as it utilizes both agents. With parameters fixed, including Q_{uv} , and concentrations of iron and peroxide. The DOC, apart from the chelating agent, is the only parameter that varies, as the results are compared for two different water matrices, MBR and CAS. Water from an MBR is of higher quality as the membranes retain smaller-sized particles, allowing better control of suspended solids, and facilitating nutrient removal. Conversely, CAS water, while of good quality, does not meet the quality standards of MBR. CAS water will require more energy to eliminate the same quantity of contaminants as MBR water. Consequently, if the same energy is utilized, CAS will exhibit lower elimination efficiencies.

Taking this into account and considering the use of different chelating agents with different stabilities between iron and the chelating agent ($k_{stab} \text{EDDS-Fe(III)} = 22.0$ $k_{stab} \text{EDTA-Fe(III)} = 25.1$), the comparison reveals significant differences in elimination efficiencies between EDDS

and EDTA. As a greater stability between iron and the chelating agent implies that the formation of complexes between them is more resilient and less prone to decomposition. This is advantageous because it helps to keep iron in solution, which is essential for the effectiveness of the photo-Fenton process. If stability is low, iron could precipitate and be lost, negatively impacting treatment efficiency [20]. At times, this principle is not systematically fulfilled; indeed, greater stability between the chelating agent and iron tends to result in higher removal. However, the water matrix composition also plays a crucial role. In other words, considering stability, as it decreases, the iron-chelating compound becomes more accessible to light and peroxide. Consequently, this leads to a more accelerated kinetics during the initial minutes of treatment. Nevertheless, there comes a point where degradation ceases, as iron precipitates. In clearer waters with lower DOC content, there is no competition, and rapid removal is achieved, even if iron precipitates. In contrast, in more contaminated waters with higher DOC content, competition arises with the possibility of iron precipitation, thereby reducing the availability of the chelating agent. In clean waters such as MBR, if the chelating agent is less stable, the impact on the process efficiency will be limited since the process is rapid. However, in more contaminated waters as CAS, it is critical for the chelating agent to be more stable to maintain consistent efficacy and prevent iron precipitation, even if this may involve longer treatment times. In this context, a less stable chelating agent may not achieve the same removal efficiencies as one with greater stability. A comparative of the efficiencies removal at different water matrix using different chelating agents is showed at Figure 11.

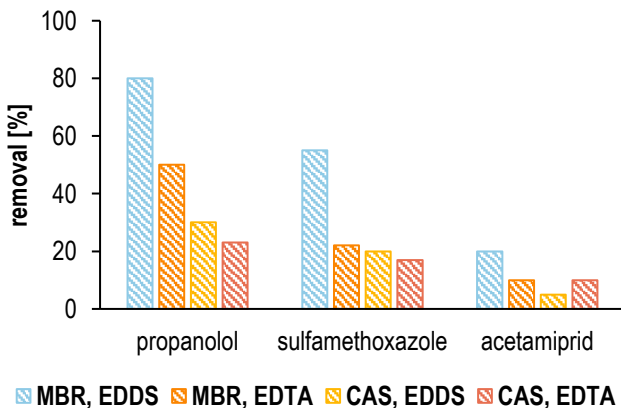


Figure 11. Comparison of elimination efficiencies with all variables fixed ($[Fe] = 0.089$ mM, $[H_2O_2] = 1.47$ mM, $DOC_{MBR} = 6.7$ mg/L, $DOC_{CAS} = 10.9$ mg/L and $Q_{UV} = 0.22$ kJ/L) except for the chelating agent.

Taking all this information into account, we observe that for cleaner water, such as in the MBR, removal is consistently higher with EDDS compared to EDTA, as previously discussed, due to differences in stabilities and their influence. With EDDS, removal rates are 80%, 55%, and 20% for propranolol, sulfamethoxazole, and acetamiprid, respectively, while with EDTA, removal rates are 50%, 22%, and 10%. It is evident that for more contaminated water, such as in the CAS, removals using one chelating agent, or the other do not vary as much. Removals using EDDS are 30%, 20%, and 5% for propranolol, sulfamethoxazole, and acetamiprid, respectively, and conversely, with EDTA, removals are 23%, 17%, and 10%. It can be observed that the use of EDDS results in higher elimination efficiencies compared to EDTA almost with all conditions. Consequently, the decision has been made to choose EDDS as the preferred chelating agent for the procedure. Additionally, this choice aligns with the current trend of regarding EDDS as a more environmentally friendly alternative to EDTA in certain circumstances [43]. The biodegradability characteristics of EDDS and its lower environmental impact contribute to its suitability as an attractive option, especially in situations where these factors are considered critical. This choice reflects the growing awareness of the environmental implications of chemical processes and underscores the importance of sustainability in decisions regarding the design and implementation of contaminant treatment.

4.1.3. Justification of the relationship between the DOC and removal efficiencies using EDDS as chelating agent.

The articles within this range employing EDDS as a chelating agent are 21, 28, 31, and 33. Due to the variability in final Q_{UV} , a calculation has been performed using the most limiting Q_{UV} for all articles and, the treatment limit time for each article can be calculated based on this limiting energy. The limiting time has been employed to determine the elimination of CECs within this time frame. Once this process is completed, the DOC can be plotted against the efficiencies, revealing a decreasing trend, as higher DOC corresponds to lower elimination.

With the examination of the preliminary graph, it is observed that there are points with higher DOC, but also high efficiencies (see Appendix 2). In article 28, the DOC has a value of 12 mg/L, and the removal efficiencies are 80% or higher, a phenomenon that lacks coherence since higher DOC content should result in lower treatment efficiency, assuming all other variables are constant. Additionally, two points are observed with a lower DOC and lower

elimination efficiencies, in article 21 and 33 the DOC has a value of 6.7 mg/L, and the removal efficiencies are 20% and 25% respectively, a situation that also lacks coherence. An analysis is undertaken to understand this anomaly, as several parameters could affect the process.

In article 28, the ratio between iron and hydrogen peroxide differs from that found in articles 21 and 33. With the remaining parameters constant, the discrepancy seems to lie here. It does not make sense for elimination efficiencies to be high such as in article 28, because acetamiprid that is a highly recalcitrant (not prone to decomposition, degradation, or elimination) CEC is being removed. A higher ratio between $\text{Fe}^{2+}/\text{H}_2\text{O}_2$ generates more hydroxyl radicals and thus increases the efficiency of the oxidation process. This ratio is higher in article 28 (0.11) than in articles 21 and 33 (0.06), justifying a higher efficiency with higher DOC on the elimination of the same CEC. The other two points on the graph that do not align are attributed to the presence of acetamiprid, which is highly recalcitrant. Consequently, the removal efficiencies are disproportionately low when the DOC is relatively small. Taking all this into account and eliminating these points, a sensible graph is obtained (Figure 12), demonstrating a decreasing trend as DOC increases, elimination efficiency decreases.

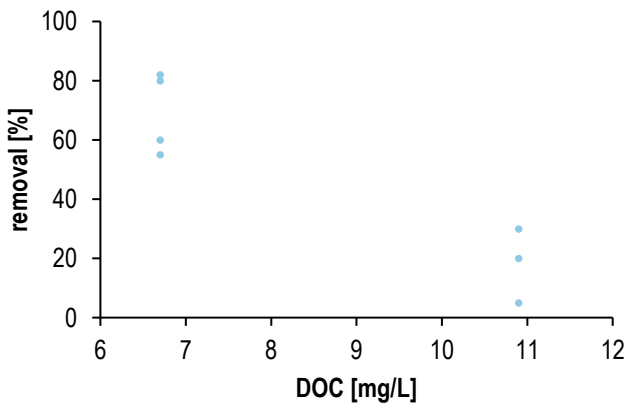


Figure 12. How does the DOC impact the elimination efficiencies of CECs when using EDDS as a chelating agent within the range 1 of artificial light.

4.1.4. Comparison of the kinetics of the different micropollutants using EDTA as chelating agent.

To compare the kinetics of the different CECs and justify the removals of them, for this type of light has been used the articles employing EDTA as a chelating agent. This decision has been made because of the information that can be extracted from the articles, although the chelating agent chosen for the process is EDDS. The articles within this range employing EDTA as a chelating agent are 21 and 33. It can be observed that, despite having the same Q_{uv} and identical concentrations of both iron and peroxide, and thus the same molar ratio, the efficiencies vary. This variability is attributed to differences in the water matrices used, employing MBR and CAS.

Comparing article 21, which utilizes an MBR matrix (DOC = 6.7 mg/L), with the results of 33, which also employs this matrix (DOC = 6.7 mg/L) under the same operating conditions and the elimination of the same contaminants, the elimination efficiencies are identical. In contrast, when comparing article 21 with the results of 33 using a CAS matrix (DOC = 10.9 mg/L), it is observed that, in article 21, the removal of propranolol is 100%, whereas in article 33, the removal of the same substance under identical conditions is 90%, elimination efficiency is lower due to a more complex water matrix and its higher DOC. In the comparison between the two matrices used in article 33, it is emphasized that the elimination efficiencies of the CAS matrix are lower due to the higher concentration of organic matter, there is increased competition between this organic matter and the CECs for the OH^\bullet . Since the removal, for example, of sulfamethoxazole in the MBR matrix is 100%, whereas in the CAS matrix, it is 75%. Therefore, with the same energy input and operating conditions, a lower percentage of microcontaminants will be eliminated, as can be seen in Figure 13.

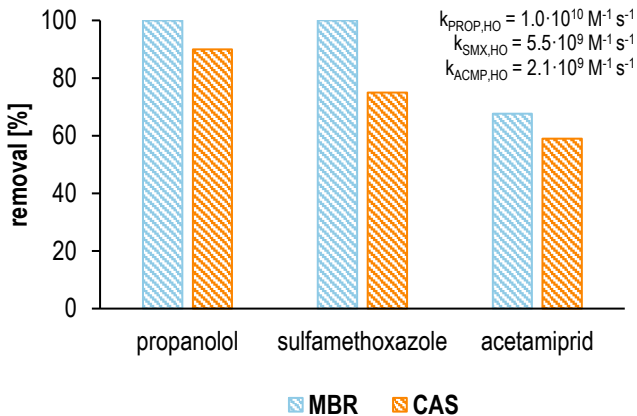


Figure 13. Elimination efficiencies of different CECs depending on the water matrix and the second order reaction rate with OH^\bullet .

Each CEC reacts differently with hydroxyl radicals, knowing that each exhibit different second order reaction rate, even under identical operating conditions, they will degrade rapidly due to their kinetics. The higher the kinetics of a compound, the greater its elimination will be. In Figure 13 it can be observed that the elimination of the CECs on a CAS matrix is 90%, 75% and 59% respectively for propranolol, sulfamethoxazole and acetaminophen. With these results it is corroborated that the higher the kinetics, the greater the removal of CECs. Also, it is observed that the removal efficiency increases when the DOC is lower (MBR < CAS).

4.2. Natural light

The process that involves artificial light requires the use of lamps and energy to ensure its operation. It is important to note that many of these lamps contain mercury, a toxic substance that can have negative impacts on human health and the environment. In this context, the EU made a significant decision on July 14, 2023, with the approval of Regulation (EU) 2023/2049, which amends Regulation (EU) 2017/852 of the European Parliament and the Council. This amendment focuses on the prohibitions of manufacturing, importing, and exporting products containing mercury. With this new regulation, the proposal is to ban the remaining intentional uses of mercury throughout the EU [48, 49]. Therefore, this regulation represents a significant

step in protecting human health and preserving the environment, given that mercury is a highly contaminating substance.

In this specific context, it is highlighted that, although it is not one of the primary objectives of the project, the decision has been made to design a facility that utilizes natural light. This choice aligns with environmental concerns and sustainability since it eliminates the need for lamps and the associated energy consumption of artificial lighting. This makes the facility eco-friendlier and contributes to the reduction of the environmental footprint associated with such technologies. Therefore, this decision not only considers European regulations on mercury but also reflects awareness of environmental issues and a commitment to more sustainable practices in the design and operation of the facility.

The articles that use natural light are 23, 24, 25, 26, 27, 30, 32, 34, 35, 36, 37, 38, 40, 43, and 44. In Table 5, it can be observed for each article the CECs that are removed, the chelating agents used for this purpose, and the concentrations of iron and peroxide.

Table 5. Main conditions of each article using natural light

n° article	CECs	Chelating agent	Iron [mM]	Peroxide [mM]
23	Caffeine, carbamazepine, propranolol, sulfamethoxazole, and trimethoprim	NTA	0.1 and 0.2	1.47 and 2.94
24	Sulfamethoxazole	EDDS	0.1	0.88
25	45 compounds, mainly pharmaceuticals, pesticides, antibiotics, and opioids	EDDS	0.1	0.88
26	Imidacloprid	NTA	0.1	1.47
27	Carbamazepine, flumequine, ibuprofen, ofloxacin, sulfamethoxazole	EDDS	0.1 and 0.2	0.8 and 1.9
30	35 compounds	EDDS	0.1 and 0.2	1.5
32	Over 60 compounds	EDDS	0.089	1.47
34	Trimethoprim	NTA	0.1 and 0.2	1.47 and 4.41
35	Caffeine, carbamazepine, diclofenac, sulfamethoxazole, and trimethoprim	EDDS	0.05 and 0.1	1.47
36	Sulfamethoxazole and imidacloprid	NTA	0.1	0.88
37	Sulfamethoxazole, pyrimicarb and imidacloprid	EDDS	0.098	0.58, 0.88 and 2.65

Continuation Table 5

<i>n° article</i>	<i>CECs</i>	<i>Chelating agent</i>	<i>Iron [mM]</i>	<i>Peroxide [mM]</i>
38	Imidacloprid	NTA	0.10 and 0.20	1.47 and 4.41
40	Lab-scale: acetaminophen, caffeine, carbamazepine, diclofenac, sulfamethoxazole, and trimethoprim; Pilot-scale: 60 compounds	EDDS	0.054 and 0.1	1.47
43	Lab-scale: acetaminophen, diclofenac, carbamazepine, caffeine, sulfamethoxazole, and trimethoprim; Pilot-scale: 46 compounds	EDDS	0.054 and 0.1	1.47
44	Caffeine, carbamazepine, diclofenac, sulfamethoxazole, and trimethoprim	EDDS	0.1	1.47

4.2.1. Selection of the optimal concentration of iron for the process using natural light.

With the aim of conducting a comprehensive analysis of the optimal parameters of the process under exposure to natural light, a segmentation methodology has been adopted for articles using it. Categorizing them into four ranges to facilitate a more thorough examination of results, based on variations in the concentrations of iron employed in the experiments. The first concentration range encompassed articles incorporating iron quantities ranging from 0 to 0.054 mM. The second range was defined for those articles implementing concentrations ranging between 0.054 and 0.098 mM. In the third range, concentrations between 0.098 and 0.1 mM were utilized, and finally, in the fourth range, articles using iron concentrations between 0.1 and 0.2 mM were included. Only the iron concentration has been considered for the definition of the ranges, as the hydrogen peroxide concentration is already included in the $\text{Fe}^{2+}/\text{H}_2\text{O}_2$ ratio. This parameter affects the process since a higher ratio generates more hydroxyl radicals and thus increases the efficiency of the oxidation process.

To choose the optimal iron concentration, a comparison of acetamidrid removal efficiencies was conducted. Acetamidrid was chosen because is a highly recalcitrant microcontaminant, all other variables were held constant.

Table 6. Comparative of the elimination efficiencies to choose the optimal range using natural light. Range 1 [Fe] = 0-0.054 mM, range 2 [Fe] = 0.054 - 0.098 mM, range 3 [Fe] = 0.098 - 0.1 mM, range 4 [Fe] = 0.1 - 0.2 mM [24].

Range 1 and 2			Range 3 and 4		
Iron [mM]	Peroxide [mM]	Removal [%]	Iron [mM]	Peroxide [mM]	Removal [%]
0.054	1.47	73	0.1	1.47	96

As evident in Table 6, the optimal iron concentration yielding higher removal efficiencies is 0.1 mM. These data also reveal that a higher ratio of iron to peroxide results as an increased removal. For instance, at a ratio of 0.03, removal is 73%, while at a ratio of 0.06, removal is 96%. This is attributed to the generation of more hydroxyl radicals at higher ratios, enhancing the oxidation process efficiency. Once the optimal iron concentration for the process is identified and the concentration range (0.098-0.1 mM) is chosen, the next step involves analysing and justifying the results obtained within this range.

4.2.2. Selection of the optimal chelating agent for the process.

In this range, the articles have been distinguished on the chelating agent employed, those utilizing EDDS and those employing NTA. Although both agents have demonstrated similar efficiencies in contaminant removal, it is noteworthy to emphasize that NTA exhibits certain advantages over the use of EDDS, such as increased stability against hydroxyl radicals and a significantly lower cost [38]. Nevertheless, despite this initial hypothesis, it is considered imperative to validate this claim and see if NTA indeed proves to be more effective in the process. The selection between the two chelating agents has been carried out in the context of the process, and this decision is grounded in the data obtained from article 36, as it utilizes both agents. With all parameters fixed, including DOC, Q_{UV} , and concentrations of iron and peroxide, the comparison reveals significant differences in elimination efficiencies between EDDS and NTA.

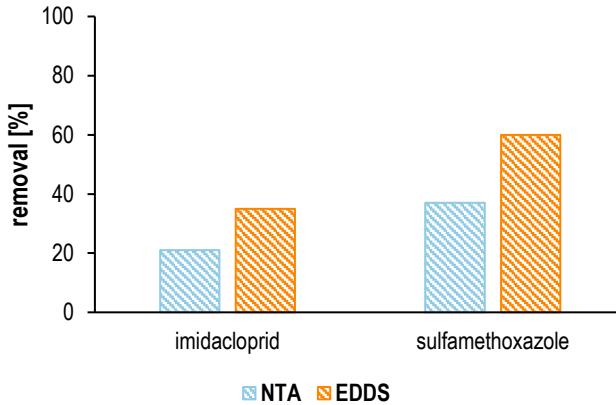


Figure 14. Comparison of elimination efficiencies with all variables fixed ($[\text{Fe}] = 0.1 \text{ mM}$, $[\text{H}_2\text{O}_2] = 0.88 \text{ mM}$, $\text{DOC} = 14.8 \text{ mg/L}$ and $Q_{\text{uv}} = 0.11 \text{ kJ/L}$) except for the chelating agent.

In Figure 14, it can be observed that the use of EDDS results in higher elimination efficiencies compared to NTA, for imidacloprid the removals are 21 % and 35% using NTA and EDDS respectively, and for sulfamethoxazole are 37% and 60%. So, the preliminary hypothesis is not fulfilled. Consequently, the decision has been made to choose EDDS as the preferred chelating agent for the procedure.

Once the optimal chelating agent for the process has been chosen, it is also necessary to consider its molar ratio with iron, as it is a parameter that impacts the efficiency of the process.

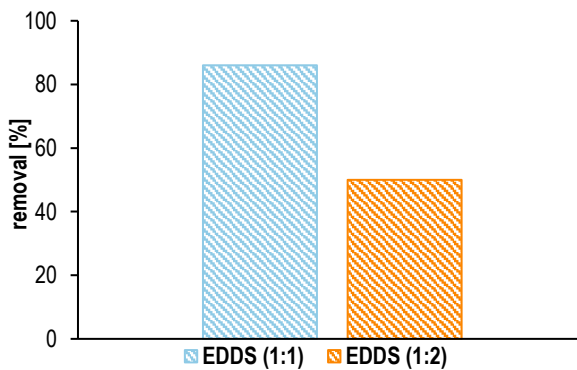


Figure 15. Comparison of the elimination efficiencies of the total MPs by varying the molar ratio between iron and EDDS.

As can be observed in Figure 15, the molar ratio that achieves higher removal, and therefore the optimal one, is 1:1. With a molar ratio of 1:1, the removal achieved is higher than 80%, though with 1:2 is only 50% [35]. This difference in efficiencies is because if the molar ratio is lower, the availability of free iron ions increases, as there is less chelating agent available to complex with iron. Additionally, the competition of the chelating agent with light and peroxide is reduced in the generation of hydroxyl radicals.

4.2.3. Natural light using EDDS (1:1) as chelating agent, comparison of the kinetics of the different micropollutants.

Each CEC reacts differently with hydroxyl radical, knowing that each exhibits different kinetics, even under identical operating conditions, they will degrade rapidly due to their kinetics [51]. The higher the kinetics of a compound, the greater its elimination will be. To substantiate this claim, the results obtained in article 35 using natural light and Fe-EDDS (1:1) have been examined.

Table 7. Reaction rate constants of hydroxyl radicals with several micropollutants.

CECs	k [M ⁻¹ ·s ⁻¹]	removal [%]
Caffeine	4.10E+09	87
Sulfamethoxazole	5.50E+09	90
Trimethoprim	8.00E+09	90
Carbamazepine	8.80E+09	100
Diclofenac	1.35E+10	100

In Table 7, it is observed that the higher the CECs kinetics, the greater its elimination. Caffeine, which is the CEC with lower kinetics ($k_{CAF,HO} = 4.10E+09 \text{ M}^{-1}\cdot\text{s}^{-1}$), achieves an 87% removal, while diclofenac, which is the CEC with higher kinetics ($k_{DCF,HO} = 1.35E+10 \text{ M}^{-1}\cdot\text{s}^{-1}$), achieves 100% removal.

Given the aim of achieving a minimum removal of 80%, it is observed that under these conditions, this target is met for the contaminant with a slower kinetics. Therefore, with 0.1 mM of iron and EDDS at a molar ratio of 1:1 with iron, this level of removal will be attained. Hence, these are the optimal conditions for the process using natural light.

4.3. Design of a raceway pond reactor with the optimal parameters for the photo-Fenton process for the wastewater treatment plant in La Jonquera

After making the sustainability-driven decision to carry out the process at the plant using natural light and having identified the optimal parameters for its execution (0.1 mM of iron, in a Fe-EDDS 1:1 ratio), we proceed to address the design phase of this installation.

The choice of opting for natural light as an energy source constitutes a strategic decision aimed at enhancing the overall sustainability of the process. This decision not only seeks to reduce dependence on non-renewable energy sources but also aims to harness the environmental benefits associated with the use of natural and renewable resources. With the optimal parameters already established, we now move on to the phase of plant design, where multiple variables will be considered to ensure the effectiveness and efficiency of the process. In this stage, the inclusion of essential components such as dosing pumps for the proper addition of iron and peroxide required for the process is anticipated. Additionally, elements such as a paddlewheel to generate water movement and a RPR are contemplated, both crucial for the operation of the photo-Fenton process. This RPR is an integral part of the plant's architecture, and its design is essential to ensure efficient water treatment. This design phase also involves specific considerations to adapt to the requirements of the La Jonquera WWTP, which must comply with the parameters and conditions previously established for the treatment plant.

Table 8. Design data of the WWTP of La Jonquera [53].

Wastewater treatment plant design data	
Treatment type	Biological treatment with nitrogen and phosphorus removal
Design flow [m ³ /day]	3,572
Equivalent population [h-e]	25,421
MES [mg/L]	330
DBO ₅ [mg/L]	427
DQO [mg/L]	870
N of design [mg/L]	65
P of design [mg/L]	10

Designing a RPR involves the meticulous consideration of various crucial factors, such as its geometry, and the availability of solar light, among other relevant considerations. Given that the operation of this wastewater treatment process depends on light, maximum importance has been assigned to this element in the reactor design process.

Two key situations are considered in relation to solar radiation: summer and winter. The variability of the Sun's position relative to the Earth in these seasons will determine the amount of radiation reaching the plant. To measure and assess this impact, a radiometer has been used to obtain specific data on radiation in the 290 to 400 nm spectrum, which is essential for the process's operation. An example of this measurement taken in Barcelona on a winter day showed a radiation level of 13.84 W/m² (Appendix 3). To contextualize this data, literature has been reviewed, revealing that radiation on winter days generally ranges between 10 and 20 W/m², while on summer days, it is between 30 and 40 W/m². Considering this information, the decision was made to base the design calculations on representative values of 15 and 35 W/m² for winter and summer days, respectively. In addition to solar radiation, other factors such as liquid depth scenarios, specifically at 5 and 15 cm, have been considered. This variation in liquid depth directly affects the distribution of light inside the reactor and, therefore, has repercussions on the efficiency of the process.

To perform the necessary calculations, it was necessary to establish a specific value of Q_{UV} , which has been effectively implemented in the context of Article 37. This decision is justified by the inclusion of this article within the range of concentrations considered optimal for the current study. The article focuses on conducting experiments involving various liquid depths, specifically 5 and 15 cm. Additionally, this choice was motivated by the elimination efficiencies of the CECs, with an average removal rate exceeding 80%. This threshold represents the minimum removal rate targeted for achievement at the plant.

Given all this, detailed calculations have been carried out for four different reactors using the equations 2 to 11. In a subsequent phase, a decision will be made regarding which of these reactors will be constructed. Thus, the reactors have been sized, yielding the following results observed at Table 9.

Table 9. Dimensions of the RPRs across different liquid depth and solar radiations scenarios. Where A_{RPR} is the total area of the reactor, R is the ratio, W is the width of the channel, L_T is the total length of the reactor and L is the length of the wall within the channels. The H represents the height of the walls, t is the width of the walls and $A_{reaction}$ is the area where the water passes.

5 cm liquid depth		15 cm liquid depth	
Sunny day	Cloudy day	Sunny day	Cloudy day
$A_{RPR} = 1,672 \text{ m}^2$	$A_{RPR} = 3,900 \text{ m}^2$	$A_{RPR} = 528 \text{ m}^2$	$A_{RPR} = 1,231 \text{ m}^2$
$R = 9 \text{ m}$	$R = 14 \text{ m}$	$R = 5 \text{ m}$	$R = 8 \text{ m}$
$W = 9 \text{ m}$	$W = 14 \text{ m}$	$W = 5 \text{ m}$	$W = 8 \text{ m}$
$L_T = 93 \text{ m}$	$L_T = 143 \text{ m}$	$L_T = 52 \text{ m}$	$L_T = 80 \text{ m}$
$L = 75 \text{ m}$	$L = 114 \text{ m}$	$L = 42 \text{ m}$	$L = 64 \text{ m}$
$H = 0.10 \text{ m}$	$H = 0.1 \text{ m}$	$H = 0.3 \text{ m}$	$H = 0.3 \text{ m}$
$t = 0.05 \text{ m}$	$t = 0.05 \text{ m}$	$t = 0.15 \text{ m}$	$t = 0.15 \text{ m}$
$A_{reaction} = 1,599 \text{ m}^2$	$A_{reaction} = 3,734 \text{ m}^2$	$A_{reaction} = 498 \text{ m}^2$	$A_{reaction} = 1,169 \text{ m}^2$

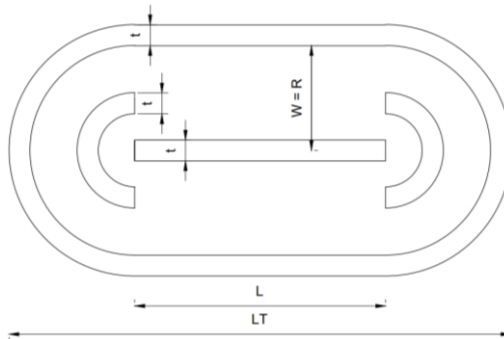


Figure 16. Schematic view of the RPR and its dimensions [own elaboration].

As observed in Table 9, in both cases of liquid depth, when the day is cloudy, more area is required. This is attributed to the diminished sunlight, and consequently, to treat the same, more space is needed to harness all the radiation that reaches the reactor in a more optimal manner. Specifically, the reaction areas on a cloudy day are slightly more than double those on a sunny day.

The objective of this study was to design an optimal reactor for carrying out the photo-Fenton process at neutral pH based on bibliographic data, and that at least an 80% removal is achieved. Once the objective is achieved, it is crucial to consider that the residence time within the reactor is 30 minutes [37] with the optimal conditions selected and a minimum removal of CECs set at 80%. Also, the design flow is set at 3572 m³/day [53]. Therefore, the entire flow will

not be treated at once. For this reason, a possible solution has been proposed, which involves installing a storage tank between the secondary and tertiary treatment stages. Given that the photo-Fenton process relies on natural light and does not operate 24 hours a day, especially during winter, the designed reactor will function from 8 am to 6 pm. Thus, it will be operational for 10 hours and inactive for 14 hours. Therefore, the tank should be designed to accommodate the water reaching the tertiary treatment during these 14 inactive hours.

Considering the non-priority nature within the scope of this study, which has been oriented as a preliminary exploration, the design of the storage tank has not been undertaken. Similarly, the pumps responsible for the pumping of reagents and the paddlewheel device have not undergone a design phase at this stage of the investigation. This decision has been made in consideration of the introductory nature of the study and its primary focus on other prioritized aspects of the process, such as the optimal parameters to carry out the process. In subsequent phases, when a more in-depth analysis of the preliminary results is conducted, the development of the design for these specific elements of the system could be considered.

4.4. Feasibility study of the raceway pond reactor at the wastewater treatment plant in La Jonquera

With the aim of determining which of the four reactors will be constructed, a criterion exclusively economic has been applied, as each of them will ensure the desired elimination. Therefore, an economic feasibility study has been conducted, considering both the cost of the RPR and the cost of the land. This meticulous analysis not only encompasses the intrinsic economic aspects of each reactor option but also incorporates the costs associated with the land, contributing to an informed and efficient decision-making process.

The decision has been made to construct the RPR with reinforced concrete, as it is an economical and, at the same time, resilient material. The cost of this, including labour, is \$890/m³ for the floor and \$1144/m³ for the walls (updated to USD 2022) [50]. Therefore, it was necessary to calculate the volume of both the floor and the walls to determine the total cost of each reactor (Table 10). The selection of concrete as the construction material is based on its economic availability and its intrinsic ability to provide a robust structure. With a specific price established for each area of the reactor. This choice is framed by the desire to ensure not only economic efficiency but also durability and resistance, key factors in the development of a

reactor that fulfils its desired functions optimally. The inclusion of labour costs ensures a realistic estimate of the financial resources required to successfully carry out the construction.

Table 10. Prices of the different RPR

5 cm liquid depth				15 cm liquid depth			
Sunny day		Cloudy day		Sunny day		Cloudy day	
$V_{\text{wall}} =$	8 m ³	$V_{\text{wall}} =$	18 m ³	$V_{\text{wall}} =$	14 m ³	$V_{\text{wall}} =$	27 m ³
$V_{\text{floor}} =$	80 m ³	$V_{\text{floor}} =$	187 m ³	$V_{\text{floor}} =$	75 m ³	$V_{\text{floor}} =$	175 m ³
$C_{\text{walls}} =$	9,549 \$	$C_{\text{walls}} =$	20,910 \$	$C_{\text{walls}} =$	16,043 \$	$C_{\text{walls}} =$	30,489 \$
$C_{\text{floor}} =$	71,136 \$	$C_{\text{floor}} =$	166,145 \$	$C_{\text{floor}} =$	66,527 \$	$C_{\text{floor}} =$	156,044 \$
$C_{\text{total}} =$	80,686 \$	$C_{\text{total}} =$	187,055 \$	$C_{\text{total}} =$	82,571 \$	$C_{\text{total}} =$	186,534 \$
$C_{\text{total}} =$	73,424 €	$C_{\text{total}} =$	170,220 €	$C_{\text{total}} =$	75,139 €	$C_{\text{total}} =$	169,746 €

As previously mentioned, the costs of the land for building the RPR have also been considered. This consideration arises due to the limited availability of space at the current treatment plant, which does not allow for the integration of the RPR without additional land acquisition. The procedure followed to accomplish this is as follows. Firstly, a thorough analysis was conducted to determine the amount of land available for the construction of the RPR at the designated location (Figure 17).



Figure 17. Disposable land on the WWTP of La Jonquera [Google Maps].

With the information about the available surface, the specific amount of land required for the construction of each of the four reactors was then calculated. Subsequently, an investigation into land prices was carried out at the Tax Agency of Catalonia. In this regard, it was identified that the type of land required for the construction of the RPR is industrial land. This specific land is part of the tenth area, situated in an industrial estate located in an area with low industrial density. Furthermore, it belongs to the first category, as it is an estate with quick access to urban centres and notable urbanization quality. With this information, it has been established

that the price per square meter of this land will be 47 € [52]. Finally, the total cost of purchasing the necessary land for each reactor has been calculated, considering the required surface and the previously established price per square meter.

Table 11. prices for the expansion of the plant for each reactor

5 cm liquid depth				15 cm liquid depth			
Sunny day		Cloudy day		Sunny day		Cloudy day	
$L_{\text{expansion}} =$	58 m	$L_{\text{expansion}} =$	108 m	$L_{\text{expansion}} =$	17 m	$L_{\text{expansion}} =$	45 m
$W_{\text{expansion}} =$	23 m	$W_{\text{expansion}} =$	23 m	$W_{\text{expansion}} =$	23 m	$W_{\text{expansion}} =$	23 m
$A_{\text{expansion}} =$	1,344 m ²	$A_{\text{expansion}} =$	2,478 m ²	$A_{\text{expansion}} =$	402 m ²	$A_{\text{expansion}} =$	1,039 m ²
$C_{\text{expansion}} =$	63,185 €	$C_{\text{expansion}} =$	116,476 €	$C_{\text{expansion}} =$	18,914 €	$C_{\text{expansion}} =$	48,851 €

The total costs consist of the sum of the RPR cost and the cost of the land to be acquired. At table 12 it can be seen the total costs for each case. It is important to note that in this analysis, only the costs associated with concrete and land have been considered. This is because costs related to personnel, pumps, paddlewheel, reagents, chelating agents, among others, would be uniform for all reactors as the treated water would be the same. Consequently, these costs would not have a significant impact on the final decision regarding which reactor to construct. As a result, they have been excluded from the scope of this preliminary study, as their inclusion would not provide relevant information at this early stage of reactor evaluation.

Table 12. Total costs of the implementation of the RPRs and the land needed to do that.

5 cm liquid depth	Sunny day	$C_{\text{RPR}} =$	73,424 €
		$C_{\text{expansion}} =$	63,185 €
	$C_{\text{total}} =$		136,609 €
	Cloudy day	$C_{\text{RPR}} =$	170,220 €
$C_{\text{expansion}} =$		116,476 €	
$C_{\text{total}} =$		286,696 €	
15 cm liquid depth	Sunny day	$C_{\text{RPR}} =$	75,139 €
		$C_{\text{expansion}} =$	18,914 €
	$C_{\text{total}} =$		94,054 €
	Cloudy day	$C_{\text{RPR}} =$	169,746 €
$C_{\text{expansion}} =$		48,851 €	
$C_{\text{total}} =$		218,597 €	

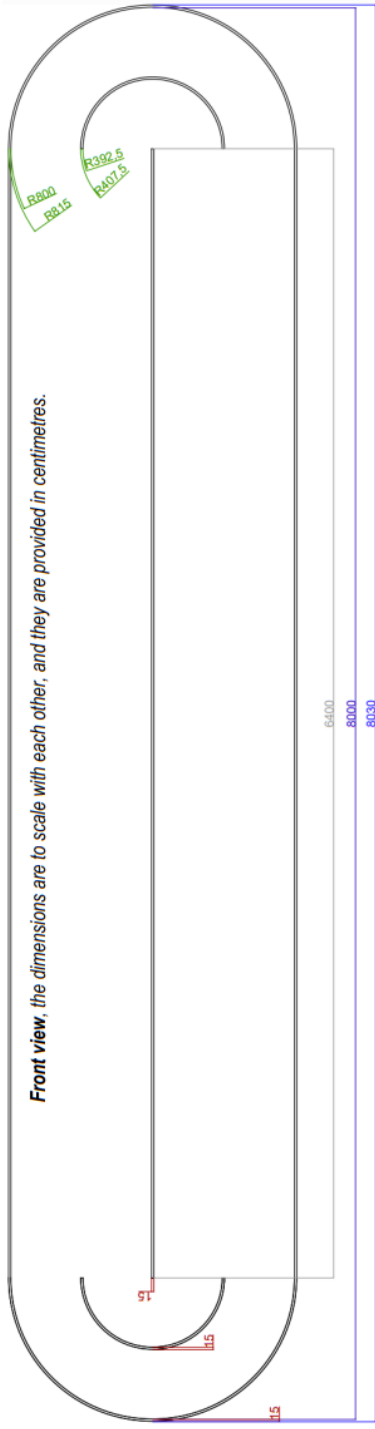
With the aim of making a choice based on economic criteria to determine which RPR will be constructed, it is observed that opting for those with a liquid depth of 15 cm results in a lower total cost, it is at least 30% lower than the cost for the reactor using a 5 cm liquid depth. Nevertheless, in the design process, it is imperative to consider the worst-case scenarios. For this reason, the design based on irradiance as if the day were cloudy will be selected. This approach ensures that, even in optimal situations with increased solar radiation, the desired elimination is effectively achieved. This choice anticipates potential challenges associated with adverse weather conditions and ensures the consistency of the RPR's performance regardless of climatic variations.

Therefore, the measures of the RPR that will be implemented at La Jonquera WWTP are those shown in Table 13, and the map of it is shown at the following page.

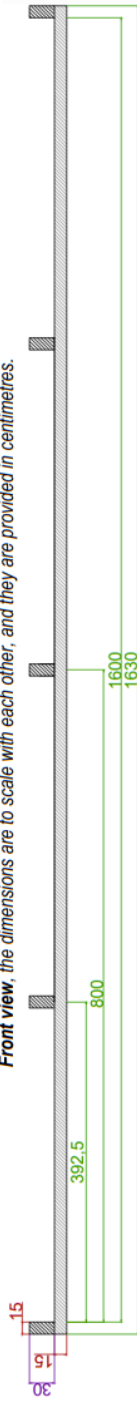
Table 13. Dimensions of the RPR for the WWTP of La Jonquera

$A_{RPR} =$	1,231	m^2	$L_T =$	80	m
$A_{reaction} =$	1,169	m^2	$L =$	64	m
$R = W =$	8	m	$H =$	0.3	m
			$t =$	0.15	m

Front view, the dimensions are to scale with each other, and they are provided in centimetres.



Front view, the dimensions are to scale with each other, and they are provided in centimetres.



Side view, because the designed reactor is quite lengthy, the measurements for representing this view are not in proportion to each other. This adjustment has been made to enhance clarity in representing and understanding the lateral view. The dimensions are provided in centimetres.



Title: Dimensioned raceway pond reactor

Print No: 1

Berta Melgar Rigau

Social reason:  UNIVERSITAT DE BARCELONA

20 / 12 / 2023

TFG

5. CONCLUSIONS

Firstly, it can be said that the photo-Fenton process at neutral pH has proven to be effective in the elimination of microcontaminants present in wastewater. Through this research, it has been verified that this method offers a viable and effective solution to treat wastewater.

On the other hand, the results obtained with the use of artificial light and natural light have revealed significant similarities. This finding suggests that the photo-Fenton process at neutral pH is robust and can be successfully implemented under various lighting conditions, providing flexibility in its practical application.

Regarding the optimal conditions for carrying out the process with natural light as a more sustainable option, it has been determined that the use of 0.1 mM of iron, 1.47 mM of hydrogen peroxide and EDDS as a chelating agent with a 1:1 molar ratio with iron offer optimized results. These conditions have been found with DOC values close to 15 mg/L (high value, worse conditions), and translate into an elimination of pollutants of more than 80%. This optimization is crucial to ensure optimal performance of the photo-Fenton process at neutral pH, contributing to its effectiveness and practical applicability.

Finally, the importance of optimizing reactor design can be highlighted. Through a systematic analysis that has included different radiation and depth conditions of the liquid, a reactor has been chosen for its construction in the WWTP of La Jonquera considering the costs of it.

All the objectives set for this work have been successfully achieved. Furthermore, with the identified optimal parameters, the feasibility of installing a raceway pond reactor in La Jonquera is affirmed. This finding supports the practical applicability of the obtained results and opens the possibility of effectively implementing the neutral pH photo-Fenton process as an efficient alternative for wastewater reuse in this WWTP.

REFERENCES AND NOTES

- [1] López-Vinent, N. (2021). Photo-Fenton at circumneutral pH for agricultural water reuse. Dipòsit Digital de la UB.
- [2] Pomázi, I. (2012). OECD Environmental Outlook to 2050: The Consequences of Inaction. *International Journal of Sustainability in Higher Education*, 13(3). <https://doi.org/10.1108/ijshe.2012.24913caa.010>
- [3] Salimi, M., Esrafil, A., Gholami, M., Jafari, A. J., Kalantary, R. R., Farzadkia, M., Kermani, M., & Sobhi, H. R. (2017). Contaminants of Emerging Concern: A review of new approach in AOP technologies. *Environmental Monitoring and Assessment*, 189(8). <https://doi.org/10.1007/s10661-017-6097-x>
- [4] Rogowska, J., Cieszyńska-Semenowicz, M., Ratajczyk, W., & Wolska, L. (2019). Micropollutants in treated wastewater. *AMBIO: A Journal of the Human Environment*, 49(2), 487-503. <https://doi.org/10.1007/s13280-019-01219-5>
- [5] Soriano-Molina P., De la Obra Jiménez I., Gualda-Alonso E., Sánchez Pérez J.A. (2020). Regeneración de aguas mediante foto-Fenton solar, una tecnología en desarrollo. RETEMA.
- [6] Directiva (CE) 2000/60 del Parlamento Europeo y del Consejo, de 23 de octubre de 2000, por la que se establece un marco comunitario de actuación en el ámbito de la política de aguas. *Diario Oficial de las Comunidades Europeas*, L 327/1, de 22 de diciembre de 2000.
- [7] Reglamento (UE) 2020/741 del Parlamento Europeo y del Consejo, de 25 de mayo de 2020, relativo a los requisitos mínimos para la reutilización del agua. *Diario Oficial de la Unión Europea*, L 177/32, de 5 de junio de 2020.
- [8] 2023. Medio Ambiente y Sostenibilidad. Gencat. Consultado en <https://mediambient.gencat.cat/es/details/Noticies/20230919-aspersor>
- [9] BOE-A-2023-11187 Consultado en [<https://www.boe.es/eli/es/rd/2023/05/11/4/con>]
- [10] Hajalifard, Z., Mousazadeh, M., Khademi, S., Khademi, N., Jamadi, M. H., Sillanpää, M. (2023). The efficacious of AOP-based processes in concert with electrocoagulation in abatement of CECs from water/wastewater. *npj Clean Water*, 6(1). <https://doi.org/10.1038/s41545-023-00239-9>
- [11] Prete, P., Fiorentino, A., Rizzo, L., Proto, A., Cucciniello, R. (2021). Review of aminopolycarboxylic acids-based metal complexes application to water and wastewater treatment by (photo-)Fenton Process at neutral pH. *Current Opinion in Green and Sustainable Chemistry*, 28, 100451. <https://doi.org/10.1016/j.cogsc.2021.100451>
- [12] Ovalle, R. (2022). A History of the Fenton Reactions (Fenton Chemistry for Beginners). *IntechOpen*. doi: 10.5772/intechopen.99846
- [13] Review: Pouran, S. R., Aziz, A., Daud, W. M. A. W. (2015). Review on the main advances in photo-Fenton oxidation system for recalcitrant wastewaters. *Journal of Industrial and Engineering Chemistry*, 21, 53-69. <https://doi.org/10.1016/j.jiec.2014.05.005>
- [14] Gualda-Alonso, E., Soriano-Molina, P., López, J. C., Sánchez, J. F. F., Plaza-Bolaños, P., Agüera, A., Pérez, J. A. S. (2022). Large-scale raceway pond reactor for CEC removal from municipal WWTP effluents by solar Photo-Fenton. *Applied Catalysis B: Environmental*, 319, 121908. <https://doi.org/10.1016/j.apcatb.2022.121908>
- [15] De La Obra, I., Ponce-Robles, L., Miralles-Cuevas, S., Oller, I., Malato, S., Pérez, J. S. (2017). Microcontaminant removal in secondary effluents by solar Photo-Fenton at circumneutral pH in Raceway Pond reactors. *Catalysis Today*, 287, 10-14. <https://doi.org/10.1016/j.cattod.2016.12.028>
- [16] Esteban García, B., Rivas, G., Arzate, S., Sánchez Pérez, J.A. (2018). Wild bacteria inactivation in WWTP secondary effluents by solar photo-Fenton at neutral pH in raceway pond reactors. *Catalysis Today*, 313, 72-78. <https://doi.org/10.1016/j.cattod.2017.10.031>

- [17] Tanveer, M., Güyer, G. T. (2013). Solar Assisted photo degradation of wastewater by compound parabolic collectors: Review of design and operational parameters. *Renewable and Sustainable Energy Reviews*, 24, 534-543. <https://doi.org/10.1016/j.rser.2013.03.053>
- [18] Cabrera-Reina, A., Miralles-Cuevas, S., Pérez, J. A. S., Salazar, R. (2021). Application of solar photo-Fenton in raceway pond reactors: a review. *Science of The Total Environment*, 800, 149653. <https://doi.org/10.1016/j.scitotenv.2021.149653>
- [19] Ferrer Guasch, Pau. (2019). Design and manufacturing of a raceway pond reactor through FFF process [Bachelor Final Project, Universitat Politècnica de Catalunya]. UPCommons. <http://hdlhandle.net/2117/176755>
- [20] López-Vinent, N., Cruz-Alcalde, A., Malvestiti, J. A., Marco, P., Giménez, J. C. M., Esplugas, S. (2020). Organic fertilizer as a chelating agent in photo-Fenton at neutral pH with LEDs for agricultural wastewater reuse: micropollutant abatement and bacterial inactivation. *Chemical Engineering Journal*, 388, 124246. <https://doi.org/10.1016/j.cej.2020.124246>.
- [21] López-Vinent, N., Cruz-Alcalde, A., Giménez, J. C. M., Esplugas, S., Sans, C. (2021). Improvement of the photo-Fenton process at natural condition of pH using organic fertilizers mixtures: Potential application to agricultural reuse of wastewater. *Applied Catalysis B-Environmental*, 290, 120066. <https://doi.org/10.1016/j.apcatb.2021.120066>
- [22] Arzate, S., Campos-Mañas, M. C., Miralles-Cuevas, S., Agüera, A., García Sánchez, J. L., Sánchez Pérez, J. A. (2020). Removal of contaminants of emerging concern by continuous flow solar photo-Fenton process at neutral pH in open reactors. *Journal of Environmental Management*, 261, 110265. <https://doi.org/10.1016/j.jenvman.2020.110265>
- [23] Gualda-Alonso, E., Pichel, N., Soriano-Molina, P., Olivares-Ligero, E., Cadena-Aponte, F.X., Agüera, A., Pérez, J. A. S., Casas López, J. L. (2023). Continuous solar photo-Fenton for wastewater reclamation in operational environment at demonstration scale. *Journal of Hazardous Materials*, 459, 132101. <https://doi.org/10.1016/j.jhazmat.2023.132101>
- [24] Soriano-Molina, P., Miralles-Cuevas, S., Esteban García, B., Plaza-Bolaños, P., Sánchez Pérez, J. A. (2021). Two strategies of solar photo-Fenton at neutral pH for the simultaneous disinfection and removal of contaminants of emerging concern. Comparative assessment in Raceway pond reactors. *Catalysis Today*, 361, 17-23. <https://doi.org/10.1016/j.cattod.2019.11.028>
- [25] Soriano-Molina, P., Plaza-Bolaños, P., Lorenzo, A., Agüera, A., García Sánchez, J. L., Malato, S., Sánchez Pérez, J. A. (2019). Assessment of solar raceway pond reactors for removal of contaminants of emerging concern by Photo-Fenton at circumneutral pH from very different municipal wastewater effluents. *Chemical Engineering Journal*, 366, 141-149. <https://doi.org/10.1016/j.cej.2019.02.074>
- [26] Soriano-Molina, P., Miralles-Cuevas, S., Oller, I., García Sánchez, J. L., Sánchez Pérez, J. A. (2021). Contribution of temperature and photon absorption on solar photo-Fenton mediated by FE3+-NTA for CEC removal in municipal wastewater. *Applied Catalysis B-Environmental*, 294, 120251. <https://doi.org/10.1016/j.apcatb.2021.120251>
- [27] Miralles-Cuevas, S., Oller, I., Sánchez Pérez, J. A., Malato, S. (2014). Removal of pharmaceuticals from MWTP effluent by nanofiltration and solar photo-Fenton using two different iron complexes at neutral pH. *Water Research*, 64, 23-31. <https://doi.org/10.1016/j.watres.2014.06.032>
- [28] Soriano-Molina, P., García Sánchez, J. L., Malato, S., Pérez-Estrada, L. A., Sánchez Pérez, J. A. (2018). Effect of volumetric rate of photon absorption on the kinetics of micropollutant removal by solar photo-Fenton with FE3+-EDDS at neutral pH. *Chemical Engineering Journal*, 331, 84-92. <https://doi.org/10.1016/j.cej.2017.08.096>
- [29] López-Vinent, N., Cruz-Alcalde, A., Gutiérrez, C., Marco, P., Giménez, J. C. M., Esplugas, S. (2020). Micropollutant removal in real WW by Photo-Fenton (circumneutral and acid pH) with BLB and LED lamps. *Chemical Engineering Journal*, 379, 122416. <https://doi.org/10.1016/j.cej.2019.122416>
- [30] Miralles-Cuevas, S., Oller, I., Agüera, A., Ponce-Robles, L., Sánchez Pérez, J. A., Malato, S. (2015). Removal of microcontaminants from MWTP effluents by combination of membrane technologies and solar photo-Fenton at neutral pH. *Catalysis Today*, 252, 78-83. <https://doi.org/10.1016/j.cattod.2014.11.015>

- [31] Hinojosa, M., Oller, I., Quiroga, J. M., Malato, S., Egea-Corbacho, A., Acevedo-Merino, A. (2023). Solar Photo-Fenton optimization at neutral pH for microcontaminant removal at pilot plant scale. *Environmental Science and Pollution Research*, 30, 96208-96218. <https://doi.org/10.21203/rs.3.rs-2340059/v1>
- [32] Klamerth, N., Malato, S., Agüera, A., Fernández-Alba, A. (2013). Photo-Fenton and modified Photo-Fenton at neutral pH for the treatment of emerging contaminants in wastewater treatment plant effluents: a comparison. *Water Research*, 47(2), 833-840. <https://doi.org/10.1016/j.watres.2012.11.008>
- [33] López-Vinent, N., Cruz-Alcalde, A., Giménez, J., Esplugas, S. (2021). Mixtures of chelating agents to enhance photo-Fenton process at natural pH: influence of wastewater matrix on micropollutant removal and bacterial inactivation. *Science of The Total Environment*, 786, 147416. <https://doi.org/10.1016/j.scitotenv.2021.147416>
- [34] Fiorentino, A., Soriano-Molina, P., Abeledo-Lameiro, M. J., De La Obra, I., Proto, A., Polo-López, M. I., Sánchez Pérez, J. A., Rizzo, L. (2022). Neutral (FE₃+NTA) and acidic (FE₂+) pH Solar Photo-Fenton vs chlorination: Effective urban wastewater disinfection does not mean control of antibiotic resistance. *Journal of Environmental Chemical Engineering*, 10(6), 108777. <https://doi.org/10.1016/j.jece.2022.108777>
- [35] Maniakova, G., Salmerón, I., Polo-López, M. I., Oller, I., Rizzo, L., Malato, S. (2021). Simultaneous removal of contaminants of emerging concern and pathogens from urban wastewater by homogeneous solar driven advanced oxidation processes. *Science of The Total Environment*, 766, 144320. <https://doi.org/10.1016/j.scitotenv.2020.144320>
- [36] Mejri, A., Soriano-Molina, P., Miralles-Cuevas, S., Sánchez Pérez, J. A. (2020). FE₃+NTA as iron source for solar photo-Fenton at neutral pH in raceway pond reactors. *Science of The Total Environment*, 736, 139617. <https://doi.org/10.1016/j.scitotenv.2020.139617>
- [37] Mejri, A., Soriano-Molina, P., Miralles-Cuevas, S., Trabelsi, I., Sánchez Pérez, J. A. (2019). Effect of liquid depth on microcontaminant removal by solar photo-Fenton with FE(III):EDDS at neutral pH in high salinity wastewater. *Environmental Science and Pollution Research*, 26 (27), 28071-28079. <https://doi.org/10.1007/s11356-019-06042-9>
- [38] Miralles-Cuevas, S., Soriano-Molina, P., De La Obra, I., Gualda-Alonso, E., Sánchez Pérez, J. A. (2021). Simultaneous bacterial inactivation and microcontaminant removal by solar photo-Fenton mediated by FE₃+NTA in WWTP secondary effluents. *Water Research*, 205, 117686. <https://doi.org/10.1016/j.watres.2021.117686>
- [39] Conde, J. J., Abelleira, S., Estévez, S., González-Rodríguez, J., Feijóo, G., Moreira, M. T. (2023). Improving the sustainability of heterogeneous fenton-based methods for micropollutant abatement by electrochemical coupling. *Journal of Environmental Management*, 332, 117308. <https://doi.org/10.1016/j.jenvman.2023.117308>
- [40] Da Costa, E. P., Roccamante, M., Plaza-Bolaños, P., Oller, I., Agüera, A., Amorim, C. C., & Malato, S. (2021). Aluminized surface to improve solar light absorption in open reactors: application for micropollutants removal in effluents from municipal wastewater treatment plants. *Science of The Total Environment*, 755, 142624. <https://doi.org/10.1016/j.scitotenv.2020.142624>
- [41] Bensalah, N., Ahmad, M. I., Boutarfaia, A. (2019). Catalytic degradation of 4-Ethylpyridine in water by heterogeneous Photo-Fenton process. *Applied sciences*, 9 (23), 5073. <https://doi.org/10.3390/app9235073>
- [42] Bilal, M., Rizwan, K., Adeel, M., Iqbal, H. M. (2022). Hydrogen-based catalyst-assisted advanced oxidation processes to mitigate emerging pharmaceutical contaminants. *International Journal of Hydrogen Energy*, 47 (45), 19555-19569. <https://doi.org/10.1016/j.ijhydene.2021.11.018>
- [43] Kowalska, K., Roccamante, M., Cabrera Reina, A., Plaza-Bolaños, P., Oller, I., Malato, S. (2021). Pilot-scale removal of microcontaminants by solar-driven photo-Fenton in treated municipal effluents: selection of operating variables based on lab-scale experiments. *Journal of Environmental Chemical Engineering*, 9 (1), 104788. <https://doi.org/10.1016/j.jece.2020.104788>

- [44] Maniakova, G., Salmerón I., Aliste, M., Polo-López, M. I., Oller, I., Malato, S., Rizzo, L. (2022). Solar photo-Fenton at circumneutral pH using FE(III)-EDDS compared to ozonation for tertiary treatment of urban wastewater: Contaminants of Emerging Concern removal and toxicity assessment. *Chemical Engineering Journal*, 431, 133474. <https://doi.org/10.1016/j.cej.2021.133474>
- [45] Tarpani, R. R. Z., Azapagic, A. (2023). Life cycle sustainability Assessment of advanced treatment techniques for urban wastewater reuse and sewage sludge resource recovery. *Science of The Total Environment*, 869, 161771. <https://doi.org/10.1016/j.scitotenv.2023.161771>
- [46] Sunyer-Caldú, A., Quintana, G., Díaz-Cruz, M. S. (2023). Factors driving PPCPs uptake by crops after wastewater irrigation and human health implications. *Environmental Research*, 237, 116923. <https://doi.org/10.1016/j.envres.2023.116923>
- [47] Guedes, P., Martins, C., Couto, N., Silva, J., Mateus, E. P., Ribeiro, A. B., Pereira, C. S. (2022). Irrigation of soil with reclaimed wastewater acts as a buffer of microbial taxonomic and functional biodiversity. *Science of The Total Environment*, 802, 149671. <https://doi.org/10.1016/j.scitotenv.2021.149671>
- [48] Reglamento Delegado (UE) 2023/2049 de la Comisión, de 14 de julio de 2023, por el que se modifica el Reglamento (UE) 2017/852 del Parlamento Europeo y del Consejo en lo que respecta a los productos con mercurio añadido sujetos a prohibiciones de fabricación, importación y exportación. *Diario Oficial de la Unión Europea*, L 236/21, de 26 de setiembre de 2023.
- [49] 2023. La CE propone revisar el Reglamento sobre mercurio para proteger a ciudadanos y medio ambiente. RETEMA, revista técnica de medio ambiente. Consultado en <https://www.retema.es/actualidad/la-ce-propone-revisar-el-reglamento-sobre-mercurio-para-proteger-del-toxico-ciudadanos-y> .
- [50] Cruz-Alcalde, A., López-Vinent, N. The economics of homogenous, ozone- and UV-based AOPs for wastewater treatment: practical guidelines based on cost engineering methods. In preparation.
- [51] Mandal, S. K. (2018). Reaction rate constants of hydroxyl radicals with micropollutants and their significance in advanced oxidation processes. *Journal of Advanced Oxidation Technologies*, 21(1), 178-195. <https://doi.org/10.26802/jaots.2017.007>
- [52] Valores básicos de los inmuebles urbanos, Agencia Tributaria de Cataluña 2023. Consultado en [<https://atc.gencat.cat/es/agencia/normativa-i-criteris/valoracions-immobiliaries/valors-basics/>]
- [53] Agencia Catalana del Agua. Consultado en [<https://aca.gencat.cat/es/inici/index.html>]

ACRONYMS

ODS – Objectius de desenvolupament sostenible

ONU – Organització de les nacions unides

OECD – Organization for Economic Cooperation and Development

BRIICS – Brazil, Russia, India, Indonesia, China, South Africa

WWTPs – Wastewater treatment plants

CECs – Contaminants of emerging concern

µg/L – Micrograms per litre

ng/L – nanograms per litre

PPCPs – Pharmaceutical and personal care products

EDCs – Endocrine-disrupting compounds

FRs – Flame retardants

ASWs – Pesticides and artificial sweeteners

AOPs – Advanced oxidation processes

EU – European union

UV – Ultraviolet

FQ – Physico-Chemical treatment

Cl – Chlorination

MBR – Membrane bioreactor

UF – Ultrafiltration

OI – Reverse osmosis

H₂O₂ – Hydrogen peroxide

Fe²⁺ or Fe³⁺ – Iron ions

OH • – Hydroxyl radical

APCAs – Aminopolycarboxylic acids

EDTA – Ethylenediaminetetraacetic acid

EDDS – Ethylenediamine-N,N'-disuccinic acid

NTA – Nitrilotriacetic acid

DTPA – Diethylene triamine pentaacetic acid

°C – Celsius degrees

IFAS – Integrated Fixed-Film Activated Sludge

CAS – Conventional Activated Sludge

CAS-NE – Conventional Activated Sludge with nutrient elimination

CPC – Compound parabolic collectors

mg/L – Milligrams per litre

RPR – Raceway Pond Reactor

€ – Euro

m² – Square meter

Q_{uv} – Accumulated energy

I – Radiation reaching the reactor surface

A – Reactor area

t – treatment time

V – Treated volume

kJ – kilojoules

J – Joule

L – Litre

s – Seconds

L_T – Total length of the reactor

L – Length of the wall

W – Width of the channels

R – Radius

π – Number pi

t – Width of the walls

H – Height of the walls

LD – Liquid depth

DOC – Dissolved organic carbon

mM – Millimolar

Fe – Iron

k_{stab} – Stability kinetic constant

m^3 – Cubic meter

h-e – Equivalent population

DBO₅ – Biochemical Oxygen Demand

DQO – Chemical Oxygen Demand

N – Nitrogen of design

P – Phosphor of design

nm – Nanometres

W – Watts

cm – Centimetres

\$ – Dollars

APPENDICES

APPENDIX 1: KEYWORDS USED FOR THE RESEARCH

"micropollutant" AND "photo-Fenton" AND "wastewater reuse" AND "neutral pH"
"micropollutants" AND "photo-Fenton" AND "wastewater reuse" AND "neutral pH"
"micropollutant" AND "photo-Fenton" AND "wastewater reuse" AND "natural pH"
"micropollutants" AND "photo-Fenton" AND "wastewater reuse" AND "natural pH"
"micropollutant" AND "photo-Fenton" AND "wastewater" AND "neutral pH"
"micropollutants" AND "photo-Fenton" AND "wastewater" AND "neutral pH"
"micropollutant" AND "photo-Fenton" AND "wastewater" AND "natural pH"
"micropollutants" AND "photo-Fenton" AND "wastewater" AND "natural pH"
"Contaminant of emerging concern" AND "photo-Fenton" AND "wastewater" AND "neutral pH"
"Contaminants of emerging concern" AND "photo-Fenton" AND "wastewater reuse" AND
"neutral pH"
"Contaminant of emerging concern" AND "photo-Fenton" AND "wastewater" AND "natural pH"
"Contaminants of emerging concern" AND "photo-Fenton" AND "wastewater reuse" AND
"natural pH"
"disinfection" AND "photo-Fenton" AND "wastewater reuse" AND "neutral pH"
"disinfection" AND "photo-Fenton" AND "wastewater" AND "neutral pH"
"disinfection" AND "contaminant of emerging concern" AND "photo-Fenton" AND "wastewater
reuse" AND "neutral pH"
"disinfection" AND "contaminant of emerging concern" AND "photo-Fenton" AND "wastewater"
AND "neutral pH"
"micropollutant" AND "photo-Fenton" AND "wastewater reuse"
"micropollutants" AND "photo-Fenton" AND "wastewater reuse"
"micropollutant" AND "photo-Fenton" AND "wastewater"
"micropollutants" AND "photo-Fenton" AND "wastewater"

“Contaminant of emerging concern” AND “photo-Fenton” AND “wastewater reuse”

“Contaminants of emerging concern” AND “photo-Fenton” AND “wastewater reuse”

“Contaminant of emerging concern” AND “photo-Fenton” AND “wastewater”

“Contaminants of emerging concern” AND “photo-Fenton” AND “wastewater”

“disinfection” AND “photo-Fenton” AND “wastewater reuse”

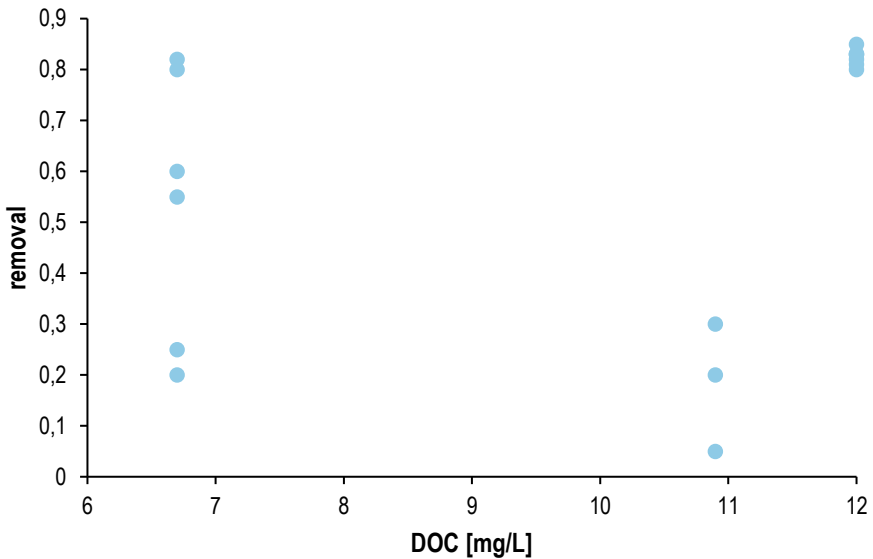
“wastewater” AND “photo-Fenton” AND “neutral pH” AND “agriculture”

“wastewater” AND “photo-Fenton” AND “neutral pH” AND “crops”

“wastewater reuse” AND “photo-Fenton” AND “neutral pH” AND “agriculture”

“wastewater reuse” AND “photo-Fenton” AND “neutral pH” AND “crops”

APPENDIX 2: PRELIMINAR GRAPH OF THE INFLUENCE FT THE DOC AT THE REMOVAL USING ARTIFICIAL LIGHT



APPENDIX 3: RADIATION MEASURED IN BERCELONA ON A WINTER DAY

λ (nm)	Mostra 1	Mostra 2	Mostra 3	Valor promig	Trapezis
290	4,95E-03	6,67E-03	5,52E-03	5,71E-03	
290,25	5,21E-03	6,58E-03	5,54E-03	5,78E-03	1,44E-03
290,5	5,58E-03	6,43E-03	5,41E-03	5,81E-03	1,45E-03
290,75	5,81E-03	6,33E-03	5,37E-03	5,83E-03	1,45E-03
291	5,56E-03	6,25E-03	5,28E-03	5,70E-03	1,44E-03
291,25	5,36E-03	6,33E-03	5,33E-03	5,67E-03	1,42E-03
291,5	5,11E-03	6,40E-03	5,50E-03	5,67E-03	1,42E-03
291,75	4,94E-03	6,47E-03	5,61E-03	5,67E-03	1,42E-03
292	5,09E-03	6,72E-03	5,74E-03	5,85E-03	1,44E-03
292,25	5,28E-03	6,54E-03	5,92E-03	5,91E-03	1,47E-03
292,5	5,31E-03	6,34E-03	5,87E-03	5,84E-03	1,47E-03
292,75	5,39E-03	6,39E-03	5,94E-03	5,91E-03	1,47E-03
293	5,41E-03	6,19E-03	5,95E-03	5,85E-03	1,47E-03
293,25	5,53E-03	6,20E-03	5,89E-03	5,87E-03	1,47E-03
293,5	5,98E-03	6,24E-03	6,04E-03	6,09E-03	1,49E-03
293,75	6,07E-03	6,35E-03	6,09E-03	6,17E-03	1,53E-03
294	6,14E-03	6,45E-03	6,10E-03	6,23E-03	1,55E-03
294,25	6,03E-03	6,61E-03	5,98E-03	6,20E-03	1,55E-03
294,5	5,77E-03	6,71E-03	5,82E-03	6,10E-03	1,54E-03
294,75	5,74E-03	6,74E-03	5,70E-03	6,06E-03	1,52E-03
295	5,79E-03	6,84E-03	5,71E-03	6,11E-03	1,52E-03
295,25	6,01E-03	6,98E-03	5,96E-03	6,32E-03	1,55E-03
295,5	6,19E-03	6,96E-03	5,96E-03	6,37E-03	1,59E-03
295,75	6,35E-03	6,86E-03	6,12E-03	6,44E-03	1,60E-03
296	6,33E-03	6,85E-03	6,23E-03	6,47E-03	1,61E-03
296,25	5,92E-03	6,68E-03	6,14E-03	6,25E-03	1,59E-03
296,5	5,68E-03	6,67E-03	6,27E-03	6,21E-03	1,56E-03

296,75	5,74E-03	6,69E-03	6,27E-03	6,23E-03	1,55E-03
297	5,95E-03	6,64E-03	6,24E-03	6,28E-03	1,56E-03
297,25	6,10E-03	6,79E-03	6,25E-03	6,38E-03	1,58E-03
297,5	6,13E-03	6,83E-03	6,16E-03	6,38E-03	1,59E-03
297,75	6,03E-03	6,94E-03	6,10E-03	6,36E-03	1,59E-03
298	5,69E-03	6,90E-03	6,00E-03	6,20E-03	1,57E-03
298,25	5,83E-03	6,96E-03	5,86E-03	6,21E-03	1,55E-03
298,5	5,99E-03	6,98E-03	5,92E-03	6,30E-03	1,56E-03
298,75	5,99E-03	6,90E-03	5,86E-03	6,25E-03	1,57E-03
299	6,18E-03	6,80E-03	5,86E-03	6,28E-03	1,57E-03
299,25	6,29E-03	6,68E-03	5,91E-03	6,29E-03	1,57E-03
299,5	6,23E-03	6,82E-03	5,97E-03	6,34E-03	1,58E-03
299,75	6,20E-03	6,89E-03	5,99E-03	6,36E-03	1,59E-03
300	6,09E-03	7,03E-03	5,99E-03	6,37E-03	1,59E-03
300,25	5,95E-03	7,14E-03	6,05E-03	6,38E-03	1,59E-03
300,5	5,88E-03	6,94E-03	6,08E-03	6,30E-03	1,59E-03
300,75	5,96E-03	6,89E-03	6,05E-03	6,30E-03	1,57E-03
301	6,00E-03	7,12E-03	6,15E-03	6,42E-03	1,59E-03
301,25	6,01E-03	7,25E-03	6,14E-03	6,47E-03	1,61E-03
301,5	6,14E-03	7,42E-03	5,95E-03	6,50E-03	1,62E-03
301,75	6,04E-03	7,38E-03	5,91E-03	6,44E-03	1,62E-03
302	6,29E-03	7,12E-03	5,77E-03	6,39E-03	1,60E-03
302,25	6,41E-03	7,05E-03	5,80E-03	6,42E-03	1,60E-03
302,5	6,42E-03	7,08E-03	6,11E-03	6,54E-03	1,62E-03
302,75	6,58E-03	7,23E-03	6,45E-03	6,75E-03	1,66E-03
303	6,54E-03	7,53E-03	6,77E-03	6,95E-03	1,71E-03
303,25	6,63E-03	7,71E-03	6,97E-03	7,10E-03	1,76E-03
303,5	6,78E-03	7,73E-03	7,09E-03	7,20E-03	1,79E-03
303,75	7,07E-03	7,83E-03	7,19E-03	7,36E-03	1,82E-03
304	7,35E-03	8,00E-03	7,57E-03	7,64E-03	1,88E-03
304,25	7,79E-03	8,38E-03	7,96E-03	8,04E-03	1,96E-03
304,5	8,27E-03	8,88E-03	8,44E-03	8,53E-03	2,07E-03
304,75	9,00E-03	9,60E-03	9,07E-03	9,22E-03	2,22E-03
305	9,54E-03	1,00E-02	9,40E-03	9,65E-03	2,36E-03
305,25	9,81E-03	1,02E-02	9,75E-03	9,92E-03	2,45E-03
305,5	9,96E-03	1,03E-02	9,98E-03	1,01E-02	2,50E-03

305,75	9,67E-03	1,02E-02	1,02E-02	1,00E-02	2,51E-03
306	9,81E-03	1,05E-02	1,04E-02	1,02E-02	2,53E-03
306,25	1,02E-02	1,11E-02	1,09E-02	1,07E-02	2,62E-03
306,5	1,09E-02	1,19E-02	1,17E-02	1,15E-02	2,78E-03
306,75	1,17E-02	1,30E-02	1,26E-02	1,24E-02	2,99E-03
307	1,28E-02	1,39E-02	1,37E-02	1,35E-02	3,24E-03
307,25	1,39E-02	1,50E-02	1,47E-02	1,45E-02	3,50E-03
307,5	1,47E-02	1,60E-02	1,55E-02	1,54E-02	3,74E-03
307,75	1,55E-02	1,67E-02	1,63E-02	1,62E-02	3,95E-03
308	1,61E-02	1,75E-02	1,70E-02	1,69E-02	4,13E-03
308,25	1,66E-02	1,78E-02	1,75E-02	1,73E-02	4,27E-03
308,5	1,68E-02	1,79E-02	1,77E-02	1,75E-02	4,35E-03
308,75	1,68E-02	1,80E-02	1,77E-02	1,75E-02	4,38E-03
309	1,70E-02	1,81E-02	1,76E-02	1,75E-02	4,39E-03
309,25	1,72E-02	1,82E-02	1,78E-02	1,77E-02	4,41E-03
309,5	1,78E-02	1,87E-02	1,82E-02	1,82E-02	4,49E-03
309,75	1,91E-02	1,98E-02	1,92E-02	1,94E-02	4,70E-03
310	2,10E-02	2,15E-02	2,15E-02	2,13E-02	5,09E-03
310,25	2,35E-02	2,42E-02	2,43E-02	2,40E-02	5,67E-03
310,5	2,63E-02	2,73E-02	2,73E-02	2,70E-02	6,38E-03
310,75	2,85E-02	2,97E-02	2,99E-02	2,94E-02	7,04E-03
311	2,99E-02	3,14E-02	3,15E-02	3,09E-02	7,53E-03
311,25	3,08E-02	3,23E-02	3,21E-02	3,17E-02	7,83E-03
311,5	3,12E-02	3,27E-02	3,23E-02	3,21E-02	7,97E-03
311,75	3,20E-02	3,36E-02	3,29E-02	3,28E-02	8,11E-03
312	3,32E-02	3,47E-02	3,38E-02	3,39E-02	8,35E-03
312,25	3,43E-02	3,60E-02	3,52E-02	3,52E-02	8,64E-03
312,5	3,56E-02	3,75E-02	3,70E-02	3,67E-02	8,98E-03
312,75	3,66E-02	3,88E-02	3,83E-02	3,79E-02	9,32E-03
313	3,72E-02	3,96E-02	3,92E-02	3,87E-02	9,57E-03
313,25	3,83E-02	4,10E-02	4,05E-02	3,99E-02	9,83E-03
313,5	3,98E-02	4,26E-02	4,21E-02	4,15E-02	1,02E-02
313,75	4,08E-02	4,34E-02	4,30E-02	4,24E-02	1,05E-02
314	4,18E-02	4,38E-02	4,36E-02	4,31E-02	1,07E-02
314,25	4,28E-02	4,44E-02	4,42E-02	4,38E-02	1,09E-02
314,5	4,37E-02	4,51E-02	4,50E-02	4,46E-02	1,11E-02

314,75	4,52E-02	4,65E-02	4,63E-02	4,60E-02	1,13E-02
315	4,60E-02	4,75E-02	4,71E-02	4,68E-02	1,16E-02
315,25	4,50E-02	4,66E-02	4,59E-02	4,58E-02	1,16E-02
315,5	4,36E-02	4,51E-02	4,44E-02	4,44E-02	1,13E-02
315,75	4,28E-02	4,43E-02	4,38E-02	4,36E-02	1,10E-02
316	4,38E-02	4,56E-02	4,51E-02	4,48E-02	1,11E-02
316,25	4,74E-02	4,95E-02	4,91E-02	4,87E-02	1,17E-02
316,5	5,23E-02	5,47E-02	5,42E-02	5,37E-02	1,28E-02
316,75	5,70E-02	5,98E-02	5,90E-02	5,86E-02	1,40E-02
317	6,06E-02	6,36E-02	6,30E-02	6,24E-02	1,51E-02
317,25	6,17E-02	6,46E-02	6,42E-02	6,35E-02	1,57E-02
317,5	6,01E-02	6,31E-02	6,25E-02	6,19E-02	1,57E-02
317,75	5,78E-02	6,08E-02	6,04E-02	5,97E-02	1,52E-02
318	5,73E-02	6,03E-02	5,93E-02	5,90E-02	1,48E-02
318,25	5,94E-02	6,24E-02	6,14E-02	6,11E-02	1,50E-02
318,5	6,26E-02	6,59E-02	6,52E-02	6,46E-02	1,57E-02
318,75	6,56E-02	6,85E-02	6,77E-02	6,72E-02	1,65E-02
319	6,67E-02	6,95E-02	6,87E-02	6,83E-02	1,69E-02
319,25	6,67E-02	6,97E-02	6,86E-02	6,83E-02	1,71E-02
319,5	6,78E-02	7,06E-02	6,96E-02	6,93E-02	1,72E-02
319,75	7,06E-02	7,38E-02	7,32E-02	7,25E-02	1,77E-02
320	7,49E-02	7,84E-02	7,78E-02	7,70E-02	1,87E-02
320,25	7,85E-02	8,18E-02	8,12E-02	8,05E-02	1,97E-02
320,5	7,96E-02	8,32E-02	8,22E-02	8,17E-02	2,03E-02
320,75	7,84E-02	8,20E-02	8,10E-02	8,05E-02	2,03E-02
321	7,62E-02	7,98E-02	7,92E-02	7,84E-02	1,99E-02
321,25	7,52E-02	7,89E-02	7,84E-02	7,75E-02	1,95E-02
321,5	7,61E-02	7,95E-02	7,91E-02	7,82E-02	1,95E-02
321,75	7,71E-02	8,06E-02	8,02E-02	7,93E-02	1,97E-02
322	7,63E-02	8,01E-02	7,93E-02	7,86E-02	1,97E-02
322,25	7,42E-02	7,85E-02	7,75E-02	7,67E-02	1,94E-02
322,5	7,27E-02	7,71E-02	7,60E-02	7,53E-02	1,90E-02
322,75	7,25E-02	7,70E-02	7,53E-02	7,49E-02	1,88E-02
323	7,53E-02	7,98E-02	7,82E-02	7,78E-02	1,91E-02
323,25	8,02E-02	8,44E-02	8,30E-02	8,26E-02	2,00E-02
323,5	8,51E-02	8,93E-02	8,87E-02	8,77E-02	2,13E-02

323,75	9,02E-02	9,48E-02	9,45E-02	9,32E-02	2,26E-02
324	9,37E-02	9,89E-02	9,84E-02	9,70E-02	2,38E-02
324,25	9,45E-02	9,99E-02	9,93E-02	9,79E-02	2,44E-02
324,5	9,45E-02	1,00E-01	9,87E-02	9,78E-02	2,45E-02
324,75	9,53E-02	1,01E-01	9,90E-02	9,83E-02	2,45E-02
325	9,81E-02	1,03E-01	1,02E-01	1,01E-01	2,49E-02
325,25	1,04E-01	1,09E-01	1,09E-01	1,08E-01	2,60E-02
325,5	1,11E-01	1,17E-01	1,16E-01	1,15E-01	2,78E-02
325,75	1,17E-01	1,24E-01	1,22E-01	1,21E-01	2,95E-02
326	1,22E-01	1,30E-01	1,27E-01	1,26E-01	3,09E-02
326,25	1,24E-01	1,32E-01	1,29E-01	1,29E-01	3,19E-02
326,5	1,25E-01	1,33E-01	1,29E-01	1,29E-01	3,22E-02
326,75	1,25E-01	1,33E-01	1,29E-01	1,29E-01	3,23E-02
327	1,23E-01	1,31E-01	1,27E-01	1,27E-01	3,20E-02
327,25	1,20E-01	1,27E-01	1,25E-01	1,24E-01	3,14E-02
327,5	1,18E-01	1,25E-01	1,23E-01	1,22E-01	3,08E-02
327,75	1,17E-01	1,22E-01	1,21E-01	1,20E-01	3,02E-02
328	1,16E-01	1,21E-01	1,20E-01	1,19E-01	2,99E-02
328,25	1,18E-01	1,24E-01	1,23E-01	1,21E-01	3,01E-02
328,5	1,24E-01	1,29E-01	1,28E-01	1,27E-01	3,10E-02
328,75	1,30E-01	1,35E-01	1,35E-01	1,34E-01	3,25E-02
329	1,38E-01	1,43E-01	1,43E-01	1,41E-01	3,43E-02
329,25	1,45E-01	1,50E-01	1,50E-01	1,48E-01	3,62E-02
329,5	1,47E-01	1,53E-01	1,52E-01	1,51E-01	3,74E-02
329,75	1,45E-01	1,52E-01	1,50E-01	1,49E-01	3,74E-02
330	1,41E-01	1,49E-01	1,46E-01	1,45E-01	3,68E-02
330,25	1,35E-01	1,44E-01	1,41E-01	1,40E-01	3,57E-02
330,5	1,31E-01	1,40E-01	1,37E-01	1,36E-01	3,45E-02
330,75	1,29E-01	1,38E-01	1,35E-01	1,34E-01	3,37E-02
331	1,29E-01	1,37E-01	1,34E-01	1,33E-01	3,34E-02
331,25	1,30E-01	1,38E-01	1,35E-01	1,34E-01	3,34E-02
331,5	1,31E-01	1,37E-01	1,35E-01	1,34E-01	3,35E-02
331,75	1,32E-01	1,38E-01	1,36E-01	1,36E-01	3,37E-02
332	1,32E-01	1,40E-01	1,38E-01	1,37E-01	3,40E-02
332,25	1,32E-01	1,40E-01	1,38E-01	1,37E-01	3,42E-02
332,5	1,32E-01	1,41E-01	1,38E-01	1,37E-01	3,43E-02

332,75	1,31E-01	1,40E-01	1,36E-01	1,36E-01	3,42E-02
333	1,29E-01	1,38E-01	1,34E-01	1,33E-01	3,37E-02
333,25	1,27E-01	1,35E-01	1,32E-01	1,31E-01	3,31E-02
333,5	1,26E-01	1,34E-01	1,31E-01	1,30E-01	3,27E-02
333,75	1,27E-01	1,36E-01	1,32E-01	1,32E-01	3,28E-02
334	1,30E-01	1,38E-01	1,35E-01	1,34E-01	3,33E-02
334,25	1,32E-01	1,40E-01	1,37E-01	1,36E-01	3,38E-02
334,5	1,34E-01	1,41E-01	1,39E-01	1,38E-01	3,43E-02
334,75	1,35E-01	1,43E-01	1,41E-01	1,39E-01	3,47E-02
335	1,35E-01	1,44E-01	1,42E-01	1,40E-01	3,50E-02
335,25	1,33E-01	1,42E-01	1,39E-01	1,38E-01	3,47E-02
335,5	1,29E-01	1,37E-01	1,34E-01	1,33E-01	3,39E-02
335,75	1,24E-01	1,33E-01	1,30E-01	1,29E-01	3,28E-02
336	1,19E-01	1,27E-01	1,25E-01	1,24E-01	3,16E-02
336,25	1,16E-01	1,24E-01	1,22E-01	1,21E-01	3,05E-02
336,5	1,14E-01	1,21E-01	1,20E-01	1,18E-01	2,99E-02
336,75	1,14E-01	1,21E-01	1,18E-01	1,18E-01	2,95E-02
337	1,15E-01	1,22E-01	1,19E-01	1,19E-01	2,96E-02
337,25	1,18E-01	1,25E-01	1,22E-01	1,22E-01	3,01E-02
337,5	1,22E-01	1,28E-01	1,25E-01	1,25E-01	3,09E-02
337,75	1,25E-01	1,32E-01	1,29E-01	1,29E-01	3,17E-02
338	1,27E-01	1,35E-01	1,32E-01	1,31E-01	3,25E-02
338,25	1,28E-01	1,37E-01	1,33E-01	1,33E-01	3,30E-02
338,5	1,30E-01	1,38E-01	1,35E-01	1,34E-01	3,34E-02
338,75	1,30E-01	1,38E-01	1,35E-01	1,34E-01	3,36E-02
339	1,30E-01	1,38E-01	1,36E-01	1,35E-01	3,36E-02
339,25	1,33E-01	1,41E-01	1,40E-01	1,38E-01	3,41E-02
339,5	1,37E-01	1,45E-01	1,43E-01	1,41E-01	3,49E-02
339,75	1,39E-01	1,48E-01	1,45E-01	1,44E-01	3,57E-02
340	1,41E-01	1,49E-01	1,47E-01	1,46E-01	3,62E-02
340,25	1,40E-01	1,49E-01	1,46E-01	1,45E-01	3,64E-02
340,5	1,39E-01	1,48E-01	1,46E-01	1,44E-01	3,62E-02
340,75	1,37E-01	1,46E-01	1,45E-01	1,43E-01	3,59E-02
341	1,36E-01	1,45E-01	1,43E-01	1,41E-01	3,55E-02
341,25	1,36E-01	1,45E-01	1,43E-01	1,41E-01	3,53E-02
341,5	1,37E-01	1,46E-01	1,44E-01	1,42E-01	3,55E-02

341,75	1,39E-01	1,48E-01	1,45E-01	1,44E-01	3,58E-02
342	1,41E-01	1,50E-01	1,47E-01	1,46E-01	3,62E-02
342,25	1,41E-01	1,51E-01	1,48E-01	1,47E-01	3,66E-02
342,5	1,41E-01	1,50E-01	1,47E-01	1,46E-01	3,66E-02
342,75	1,41E-01	1,50E-01	1,47E-01	1,46E-01	3,65E-02
343	1,40E-01	1,49E-01	1,46E-01	1,45E-01	3,64E-02
343,25	1,38E-01	1,46E-01	1,44E-01	1,43E-01	3,60E-02
343,5	1,33E-01	1,41E-01	1,38E-01	1,37E-01	3,50E-02
343,75	1,27E-01	1,36E-01	1,33E-01	1,32E-01	3,37E-02
344	1,21E-01	1,29E-01	1,26E-01	1,25E-01	3,22E-02
344,25	1,18E-01	1,26E-01	1,23E-01	1,22E-01	3,10E-02
344,5	1,19E-01	1,27E-01	1,24E-01	1,23E-01	3,07E-02
344,75	1,23E-01	1,31E-01	1,29E-01	1,28E-01	3,14E-02
345	1,28E-01	1,37E-01	1,35E-01	1,33E-01	3,26E-02
345,25	1,33E-01	1,42E-01	1,39E-01	1,38E-01	3,39E-02
345,5	1,35E-01	1,45E-01	1,42E-01	1,40E-01	3,48E-02
345,75	1,35E-01	1,45E-01	1,42E-01	1,41E-01	3,51E-02
346	1,34E-01	1,45E-01	1,41E-01	1,40E-01	3,51E-02
346,25	1,35E-01	1,46E-01	1,42E-01	1,41E-01	3,51E-02
346,5	1,37E-01	1,48E-01	1,43E-01	1,42E-01	3,54E-02
346,75	1,37E-01	1,48E-01	1,44E-01	1,43E-01	3,57E-02
347	1,36E-01	1,48E-01	1,44E-01	1,43E-01	3,57E-02
347,25	1,36E-01	1,47E-01	1,43E-01	1,42E-01	3,56E-02
347,5	1,35E-01	1,46E-01	1,42E-01	1,41E-01	3,54E-02
347,75	1,36E-01	1,47E-01	1,43E-01	1,42E-01	3,54E-02
348	1,37E-01	1,48E-01	1,44E-01	1,43E-01	3,57E-02
348,25	1,38E-01	1,50E-01	1,45E-01	1,44E-01	3,60E-02
348,5	1,38E-01	1,49E-01	1,45E-01	1,44E-01	3,60E-02
348,75	1,37E-01	1,48E-01	1,44E-01	1,43E-01	3,59E-02
349	1,36E-01	1,47E-01	1,43E-01	1,42E-01	3,56E-02
349,25	1,36E-01	1,46E-01	1,43E-01	1,42E-01	3,55E-02
349,5	1,38E-01	1,48E-01	1,45E-01	1,44E-01	3,57E-02
349,75	1,42E-01	1,53E-01	1,48E-01	1,48E-01	3,64E-02
350	1,46E-01	1,57E-01	1,54E-01	1,52E-01	3,75E-02
350,25	1,51E-01	1,62E-01	1,59E-01	1,57E-01	3,87E-02
350,5	1,53E-01	1,64E-01	1,61E-01	1,59E-01	3,95E-02

350,75	1,52E-01	1,64E-01	1,60E-01	1,59E-01	3,98E-02
351	1,51E-01	1,63E-01	1,59E-01	1,58E-01	3,96E-02
351,25	1,50E-01	1,61E-01	1,57E-01	1,56E-01	3,92E-02
351,5	1,49E-01	1,61E-01	1,56E-01	1,55E-01	3,89E-02
351,75	1,47E-01	1,59E-01	1,55E-01	1,54E-01	3,86E-02
352	1,46E-01	1,58E-01	1,54E-01	1,53E-01	3,83E-02
352,25	1,45E-01	1,57E-01	1,53E-01	1,51E-01	3,80E-02
352,5	1,46E-01	1,58E-01	1,54E-01	1,53E-01	3,80E-02
352,75	1,49E-01	1,60E-01	1,56E-01	1,55E-01	3,85E-02
353	1,53E-01	1,65E-01	1,61E-01	1,60E-01	3,94E-02
353,25	1,58E-01	1,71E-01	1,67E-01	1,65E-01	4,06E-02
353,5	1,62E-01	1,76E-01	1,71E-01	1,70E-01	4,19E-02
353,75	1,66E-01	1,81E-01	1,76E-01	1,75E-01	4,30E-02
354	1,70E-01	1,85E-01	1,80E-01	1,78E-01	4,41E-02
354,25	1,72E-01	1,86E-01	1,80E-01	1,79E-01	4,47E-02
354,5	1,72E-01	1,86E-01	1,80E-01	1,79E-01	4,48E-02
354,75	1,69E-01	1,83E-01	1,78E-01	1,77E-01	4,45E-02
355	1,68E-01	1,82E-01	1,76E-01	1,75E-01	4,40E-02
355,25	1,66E-01	1,80E-01	1,75E-01	1,74E-01	4,36E-02
355,5	1,64E-01	1,78E-01	1,72E-01	1,71E-01	4,31E-02
355,75	1,63E-01	1,76E-01	1,70E-01	1,70E-01	4,26E-02
356	1,59E-01	1,71E-01	1,66E-01	1,65E-01	4,19E-02
356,25	1,52E-01	1,65E-01	1,61E-01	1,59E-01	4,06E-02
356,5	1,47E-01	1,59E-01	1,55E-01	1,54E-01	3,91E-02
356,75	1,42E-01	1,55E-01	1,51E-01	1,49E-01	3,79E-02
357	1,40E-01	1,52E-01	1,48E-01	1,47E-01	3,70E-02
357,25	1,38E-01	1,51E-01	1,46E-01	1,45E-01	3,65E-02
357,5	1,35E-01	1,47E-01	1,43E-01	1,42E-01	3,58E-02
357,75	1,30E-01	1,42E-01	1,38E-01	1,37E-01	3,48E-02
358	1,26E-01	1,36E-01	1,33E-01	1,31E-01	3,35E-02
358,25	1,23E-01	1,34E-01	1,31E-01	1,29E-01	3,26E-02
358,5	1,25E-01	1,35E-01	1,32E-01	1,31E-01	3,25E-02
358,75	1,31E-01	1,41E-01	1,37E-01	1,37E-01	3,34E-02
359	1,41E-01	1,52E-01	1,48E-01	1,47E-01	3,55E-02
359,25	1,50E-01	1,61E-01	1,57E-01	1,56E-01	3,79E-02
359,5	1,57E-01	1,69E-01	1,65E-01	1,64E-01	4,00E-02

359,75	1,61E-01	1,74E-01	1,70E-01	1,68E-01	4,15E-02
360	1,59E-01	1,72E-01	1,68E-01	1,66E-01	4,18E-02
360,25	1,56E-01	1,69E-01	1,64E-01	1,63E-01	4,12E-02
360,5	1,52E-01	1,65E-01	1,60E-01	1,59E-01	4,02E-02
360,75	1,48E-01	1,61E-01	1,56E-01	1,55E-01	3,92E-02
361	1,46E-01	1,59E-01	1,53E-01	1,53E-01	3,85E-02
361,25	1,44E-01	1,57E-01	1,52E-01	1,51E-01	3,80E-02
361,5	1,43E-01	1,56E-01	1,51E-01	1,50E-01	3,77E-02
361,75	1,45E-01	1,58E-01	1,53E-01	1,52E-01	3,78E-02
362	1,51E-01	1,63E-01	1,58E-01	1,57E-01	3,87E-02
362,25	1,56E-01	1,69E-01	1,65E-01	1,63E-01	4,01E-02
362,5	1,61E-01	1,75E-01	1,70E-01	1,69E-01	4,15E-02
362,75	1,65E-01	1,79E-01	1,74E-01	1,72E-01	4,27E-02
363	1,64E-01	1,78E-01	1,73E-01	1,72E-01	4,30E-02
363,25	1,64E-01	1,78E-01	1,73E-01	1,72E-01	4,29E-02
363,5	1,65E-01	1,79E-01	1,74E-01	1,73E-01	4,31E-02
363,75	1,64E-01	1,79E-01	1,74E-01	1,72E-01	4,32E-02
364	1,65E-01	1,79E-01	1,75E-01	1,73E-01	4,32E-02
364,25	1,65E-01	1,79E-01	1,74E-01	1,73E-01	4,32E-02
364,5	1,66E-01	1,80E-01	1,75E-01	1,73E-01	4,33E-02
364,75	1,69E-01	1,84E-01	1,79E-01	1,77E-01	4,38E-02
365	1,75E-01	1,91E-01	1,85E-01	1,84E-01	4,51E-02
365,25	1,82E-01	1,99E-01	1,93E-01	1,92E-01	4,69E-02
365,5	1,89E-01	2,08E-01	2,01E-01	1,99E-01	4,89E-02
365,75	1,95E-01	2,13E-01	2,07E-01	2,05E-01	5,06E-02
366	1,97E-01	2,16E-01	2,09E-01	2,07E-01	5,15E-02
366,25	1,97E-01	2,15E-01	2,10E-01	2,08E-01	5,19E-02
366,5	1,97E-01	2,14E-01	2,09E-01	2,06E-01	5,17E-02
366,75	1,97E-01	2,14E-01	2,08E-01	2,06E-01	5,16E-02
367	1,97E-01	2,14E-01	2,08E-01	2,06E-01	5,16E-02
367,25	1,94E-01	2,11E-01	2,05E-01	2,04E-01	5,12E-02
367,5	1,92E-01	2,09E-01	2,02E-01	2,01E-01	5,06E-02
367,75	1,88E-01	2,05E-01	1,98E-01	1,97E-01	4,98E-02
368	1,84E-01	2,00E-01	1,95E-01	1,93E-01	4,87E-02
368,25	1,83E-01	2,00E-01	1,94E-01	1,93E-01	4,82E-02
368,5	1,84E-01	2,02E-01	1,95E-01	1,94E-01	4,83E-02

368,75	1,87E-01	2,05E-01	1,98E-01	1,97E-01	4,88E-02
369	1,91E-01	2,09E-01	2,02E-01	2,01E-01	4,97E-02
369,25	1,97E-01	2,15E-01	2,08E-01	2,06E-01	5,09E-02
369,5	1,99E-01	2,17E-01	2,10E-01	2,09E-01	5,19E-02
369,75	2,00E-01	2,18E-01	2,11E-01	2,10E-01	5,23E-02
370	1,97E-01	2,15E-01	2,08E-01	2,07E-01	5,21E-02
370,25	1,92E-01	2,09E-01	2,02E-01	2,01E-01	5,10E-02
370,5	1,91E-01	2,08E-01	2,01E-01	2,00E-01	5,01E-02
370,75	1,90E-01	2,08E-01	2,01E-01	2,00E-01	5,00E-02
371	1,92E-01	2,10E-01	2,03E-01	2,02E-01	5,02E-02
371,25	1,93E-01	2,11E-01	2,05E-01	2,03E-01	5,06E-02
371,5	1,90E-01	2,09E-01	2,02E-01	2,00E-01	5,04E-02
371,75	1,87E-01	2,05E-01	1,99E-01	1,97E-01	4,97E-02
372	1,84E-01	2,02E-01	1,96E-01	1,94E-01	4,89E-02
372,25	1,84E-01	2,02E-01	1,95E-01	1,94E-01	4,85E-02
372,5	1,82E-01	1,99E-01	1,92E-01	1,91E-01	4,81E-02
372,75	1,76E-01	1,92E-01	1,86E-01	1,85E-01	4,69E-02
373	1,70E-01	1,86E-01	1,80E-01	1,78E-01	4,54E-02
373,25	1,65E-01	1,81E-01	1,75E-01	1,74E-01	4,40E-02
373,5	1,63E-01	1,79E-01	1,73E-01	1,71E-01	4,31E-02
373,75	1,63E-01	1,79E-01	1,74E-01	1,72E-01	4,29E-02
374	1,63E-01	1,79E-01	1,74E-01	1,72E-01	4,30E-02
374,25	1,62E-01	1,79E-01	1,73E-01	1,71E-01	4,29E-02
374,5	1,62E-01	1,79E-01	1,72E-01	1,71E-01	4,28E-02
374,75	1,66E-01	1,82E-01	1,75E-01	1,74E-01	4,32E-02
375	1,71E-01	1,87E-01	1,80E-01	1,79E-01	4,42E-02
375,25	1,75E-01	1,92E-01	1,85E-01	1,84E-01	4,54E-02
375,5	1,79E-01	1,96E-01	1,90E-01	1,88E-01	4,65E-02
375,75	1,80E-01	1,98E-01	1,91E-01	1,90E-01	4,73E-02
376	1,81E-01	2,00E-01	1,93E-01	1,91E-01	4,77E-02
376,25	1,82E-01	2,01E-01	1,94E-01	1,92E-01	4,80E-02
376,5	1,86E-01	2,05E-01	1,97E-01	1,96E-01	4,86E-02
376,75	1,91E-01	2,10E-01	2,03E-01	2,01E-01	4,96E-02
377	1,98E-01	2,17E-01	2,10E-01	2,08E-01	5,12E-02
377,25	2,06E-01	2,26E-01	2,18E-01	2,17E-01	5,31E-02
377,5	2,14E-01	2,35E-01	2,27E-01	2,25E-01	5,52E-02

377,75	2,17E-01	2,38E-01	2,31E-01	2,29E-01	5,67E-02
378	2,16E-01	2,37E-01	2,30E-01	2,28E-01	5,70E-02
378,25	2,13E-01	2,34E-01	2,28E-01	2,25E-01	5,66E-02
378,5	2,08E-01	2,28E-01	2,22E-01	2,19E-01	5,55E-02
378,75	2,01E-01	2,21E-01	2,15E-01	2,12E-01	5,40E-02
379	1,94E-01	2,13E-01	2,06E-01	2,04E-01	5,21E-02
379,25	1,87E-01	2,05E-01	1,98E-01	1,97E-01	5,01E-02
379,5	1,84E-01	2,01E-01	1,95E-01	1,93E-01	4,88E-02
379,75	1,83E-01	2,01E-01	1,94E-01	1,93E-01	4,83E-02
380	1,88E-01	2,07E-01	2,00E-01	1,99E-01	4,90E-02
380,25	1,95E-01	2,16E-01	2,08E-01	2,06E-01	5,06E-02
380,5	1,99E-01	2,20E-01	2,12E-01	2,11E-01	5,21E-02
380,75	1,99E-01	2,20E-01	2,12E-01	2,10E-01	5,26E-02
381	1,95E-01	2,16E-01	2,08E-01	2,07E-01	5,21E-02
381,25	1,89E-01	2,09E-01	2,02E-01	2,00E-01	5,08E-02
381,5	1,81E-01	2,00E-01	1,93E-01	1,91E-01	4,89E-02
381,75	1,72E-01	1,90E-01	1,84E-01	1,82E-01	4,67E-02
382	1,64E-01	1,81E-01	1,75E-01	1,73E-01	4,44E-02
382,25	1,56E-01	1,72E-01	1,66E-01	1,65E-01	4,22E-02
382,5	1,47E-01	1,63E-01	1,56E-01	1,55E-01	4,00E-02
382,75	1,40E-01	1,56E-01	1,49E-01	1,48E-01	3,79E-02
383	1,35E-01	1,49E-01	1,43E-01	1,42E-01	3,63E-02
383,25	1,32E-01	1,46E-01	1,40E-01	1,39E-01	3,52E-02
383,5	1,34E-01	1,48E-01	1,43E-01	1,42E-01	3,51E-02
383,75	1,41E-01	1,55E-01	1,50E-01	1,49E-01	3,63E-02
384	1,50E-01	1,66E-01	1,59E-01	1,58E-01	3,84E-02
384,25	1,61E-01	1,78E-01	1,71E-01	1,70E-01	4,10E-02
384,5	1,69E-01	1,87E-01	1,79E-01	1,78E-01	4,35E-02
384,75	1,73E-01	1,92E-01	1,85E-01	1,83E-01	4,52E-02
385	1,74E-01	1,93E-01	1,86E-01	1,85E-01	4,60E-02
385,25	1,74E-01	1,93E-01	1,86E-01	1,84E-01	4,61E-02
385,5	1,72E-01	1,91E-01	1,85E-01	1,83E-01	4,59E-02
385,75	1,73E-01	1,92E-01	1,85E-01	1,83E-01	4,57E-02
386	1,75E-01	1,93E-01	1,87E-01	1,85E-01	4,60E-02
386,25	1,78E-01	1,96E-01	1,89E-01	1,87E-01	4,66E-02
386,5	1,80E-01	1,97E-01	1,90E-01	1,89E-01	4,71E-02

386,75	1,80E-01	1,98E-01	1,91E-01	1,90E-01	4,73E-02
387	1,79E-01	1,97E-01	1,90E-01	1,89E-01	4,73E-02
387,25	1,78E-01	1,97E-01	1,89E-01	1,88E-01	4,71E-02
387,5	1,77E-01	1,96E-01	1,88E-01	1,87E-01	4,69E-02
387,75	1,76E-01	1,94E-01	1,86E-01	1,85E-01	4,65E-02
388	1,75E-01	1,93E-01	1,86E-01	1,84E-01	4,62E-02
388,25	1,74E-01	1,92E-01	1,84E-01	1,83E-01	4,60E-02
388,5	1,77E-01	1,95E-01	1,88E-01	1,87E-01	4,63E-02
388,75	1,82E-01	2,01E-01	1,93E-01	1,92E-01	4,74E-02
389	1,90E-01	2,10E-01	2,01E-01	2,00E-01	4,90E-02
389,25	1,99E-01	2,20E-01	2,10E-01	2,09E-01	5,12E-02
389,5	2,06E-01	2,28E-01	2,18E-01	2,17E-01	5,33E-02
389,75	2,12E-01	2,36E-01	2,25E-01	2,24E-01	5,52E-02
390	2,17E-01	2,41E-01	2,31E-01	2,30E-01	5,67E-02
390,25	2,21E-01	2,45E-01	2,35E-01	2,34E-01	5,79E-02
390,5	2,27E-01	2,51E-01	2,41E-01	2,40E-01	5,92E-02
390,75	2,32E-01	2,56E-01	2,46E-01	2,45E-01	6,05E-02
391	2,34E-01	2,59E-01	2,49E-01	2,47E-01	6,15E-02
391,25	2,33E-01	2,57E-01	2,48E-01	2,46E-01	6,16E-02
391,5	2,29E-01	2,52E-01	2,43E-01	2,41E-01	6,09E-02
391,75	2,19E-01	2,42E-01	2,34E-01	2,32E-01	5,91E-02
392	2,07E-01	2,29E-01	2,21E-01	2,19E-01	5,64E-02
392,25	1,92E-01	2,13E-01	2,05E-01	2,03E-01	5,28E-02
392,5	1,71E-01	1,90E-01	1,82E-01	1,81E-01	4,80E-02
392,75	1,51E-01	1,68E-01	1,61E-01	1,60E-01	4,27E-02
393	1,37E-01	1,52E-01	1,46E-01	1,45E-01	3,81E-02
393,25	1,31E-01	1,45E-01	1,39E-01	1,38E-01	3,54E-02
393,5	1,35E-01	1,49E-01	1,43E-01	1,42E-01	3,51E-02
393,75	1,46E-01	1,62E-01	1,55E-01	1,54E-01	3,70E-02
394	1,62E-01	1,80E-01	1,72E-01	1,71E-01	4,07E-02
394,25	1,79E-01	1,99E-01	1,91E-01	1,90E-01	4,51E-02
394,5	1,95E-01	2,17E-01	2,08E-01	2,07E-01	4,95E-02
394,75	2,09E-01	2,33E-01	2,23E-01	2,22E-01	5,36E-02
395	2,20E-01	2,45E-01	2,35E-01	2,34E-01	5,69E-02
395,25	2,24E-01	2,50E-01	2,40E-01	2,38E-01	5,90E-02
395,5	2,21E-01	2,46E-01	2,36E-01	2,34E-01	5,90E-02

395,75	2,12E-01	2,36E-01	2,27E-01	2,25E-01	5,74E-02
396	1,97E-01	2,20E-01	2,11E-01	2,09E-01	5,43E-02
396,25	1,81E-01	2,02E-01	1,94E-01	1,92E-01	5,02E-02
396,5	1,70E-01	1,89E-01	1,81E-01	1,80E-01	4,66E-02
396,75	1,66E-01	1,84E-01	1,76E-01	1,76E-01	4,45E-02
397	1,72E-01	1,91E-01	1,83E-01	1,82E-01	4,47E-02
397,25	1,85E-01	2,06E-01	1,97E-01	1,96E-01	4,73E-02
397,5	2,01E-01	2,23E-01	2,14E-01	2,13E-01	5,11E-02
397,75	2,18E-01	2,43E-01	2,33E-01	2,32E-01	5,55E-02
398	2,31E-01	2,57E-01	2,47E-01	2,45E-01	5,95E-02
398,25	2,41E-01	2,67E-01	2,57E-01	2,55E-01	6,25E-02
398,5	2,51E-01	2,79E-01	2,67E-01	2,66E-01	6,51E-02
398,75	2,58E-01	2,86E-01	2,74E-01	2,73E-01	6,73E-02
399	2,63E-01	2,93E-01	2,80E-01	2,79E-01	6,89E-02
399,25	2,70E-01	3,00E-01	2,88E-01	2,86E-01	7,06E-02
399,5	2,74E-01	3,04E-01	2,91E-01	2,90E-01	7,20E-02
399,75	2,78E-01	3,08E-01	2,95E-01	2,93E-01	7,29E-02
400	2,81E-01	3,11E-01	2,98E-01	2,97E-01	7,38E-02

TOTAL = 13,84 W/m²

